Springer Theses
Recognizing Outstanding Ph.D. Research

Jing Yu

Adhesive Interactions of Mussel Foot Proteins

Springer

Springer Theses

Recognizing Outstanding Ph.D. Research

For further volumes:
http://www.springer.com/series/8790

Aims and Scope

The series "Springer Theses" brings together a selection of the very best Ph.D. theses from around the world and across the physical sciences. Nominated and endorsed by two recognized specialists, each published volume has been selected for its scientific excellence and the high impact of its contents for the pertinent field of research. For greater accessibility to non-specialists, the published versions include an extended introduction, as well as a foreword by the student's supervisor explaining the special relevance of the work for the field. As a whole, the series will provide a valuable resource both for newcomers to the research fields described, and for other scientists seeking detailed background information on special questions. Finally, it provides an accredited documentation of the valuable contributions made by today's younger generation of scientists.

Theses are accepted into the series by invited nomination only and must fulfill all of the following criteria

- They must be written in good English.
- The topic should fall within the confines of Chemistry, Physics, Earth Sciences, Engineering and related interdisciplinary fields such as Materials, Nanoscience, Chemical Engineering, Complex Systems and Biophysics.
- The work reported in the thesis must represent a significant scientific advance.
- If the thesis includes previously published material, permission to reproduce this must be gained from the respective copyright holder.
- They must have been examined and passed during the 12 months prior to nomination.
- Each thesis should include a foreword by the supervisor outlining the significance of its content.
- The theses should have a clearly defined structure including an introduction accessible to scientists not expert in that particular field.

Jing Yu

Adhesive Interactions of Mussel Foot Proteins

Springer

Jing Yu
California Institute of Technology
Pasadena, CA, USA

ISSN 2190-5053 ISSN 2190-5061 (electronic)
ISBN 978-3-319-06030-9 ISBN 978-3-319-06031-6 (eBook)
DOI 10.1007/978-3-319-06031-6
Springer Cham Heidelberg New York Dordrecht London

Library of Congress Control Number: 2014940169

Printed on acid-free paper

Springer is part of Springer Science+Business Media (www.springer.com)

Series Information Text

Springer Theses – the "best of the best"

Internationally top-ranked research institutes select their best thesis annually for publication in this series. Nominated and endorsed by two recognized specialists, each thesis is chosen for its scientific excellence and impact on research. For greater accessibility to non-specialists, the published versions include an extended introduction, as well as a foreword by the student's supervisor explaining the special relevance of the work for the field. As a whole, the series provides a valuable resource both for newcomers to the relevant field, and for other scientists seeking detailed background information on special questions. Finally, it provides an accredited documentation of the valuable contributions made by today's younger generation of scientists.

The content of the series is available to millions of readers worldwide and, in addition to profiting from this broad dissemination, the author of each thesis is rewarded with a cash prize equivalent to € 500.

Foreword

Dr. Jing Yu conducted and pioneered outstanding research in many important areas including the wet adhesion of marine mussel adhesive proteins (his thesis topic), but also the reversible dry adhesion of geckos, and the biolubrication mechanism of human joints.

Dr. Yu's thesis research was devoted to elucidating the adhesive mechanisms of protein-based adhesives inspired by marine mussels, which can strongly adhere to different surfaces even in highly contaminated water and even when surfaces are covered by contaminant layers, known as "biofilms." Adhesives that work in such adverse conditions are in high demand, especially in the medical field, as dental adhesives, and for sealing tissues, for example, after surgery. The US market for medical adhesives and sealants is forecast to exceed $2 billion by the year 2017. However, existing tissue adhesives suffer from weak adhesive strength due to the presence of water and certain common organic or inorganic solutes, which severely limit their current adhesive applications. To overcome this problem, we look to nature, as marine mussels use protein-based adhesives to strongly and stably attach themselves to various wet surfaces in the ocean. Understanding the mechanism behind this natural, strong, moisture-resistant adhesive action is critical for designing novel medical adhesives.

Previously, little was known about the molecular mechanism of mussel adhesion. Using a surface forces apparatus (SFA) and other physicochemical techniques, Yu was the first person worldwide to conduct a detailed study of the molecular-binding (adhesion) mechanisms of marine mussel adhesive proteins on various surfaces, including mica, titanium dioxide, and thin organic films, and identified and clarified the crucial role of the double hydrogen-bonding group, L-3,4-dihydroxyphenylalanine (commonly known as Dopa) in the bonding mechanism. More specifically, he discovered that the surface redox of Dopa is extremely important for its adhesive properties. Dopa is not very stable at the pH of the human body, which prevents the wide use of Dopa-containing polymers as medical adhesives. However, Dr. Yu found that mussels make use of this property by imposing an acidic, low pH, regime in the confined space where the mussel secretes the adhesion protein.

Dr. Yu's research on mussel-inspired adhesives has had a profound affect worldwide; his work has been cited many times internationally and has also drawn the attention of multiple international journals and online media sources including *Nature Chemical Biology*, *ABC Science,* and the *Faculty of 1000*. His work lays the foundation for developing mussel-inspired adhesives and biomimetic coatings for a wide range of biomedical applications such as cell encapsulants, bone/dental glues, paints for coronary arteries, fetal membrane sealants, and organ transplants.

Santa Barbara, CA, USA Jacob Israelachvili

Preface

Improving our understanding of wet adhesion is crucial for developing the next generation of wet adhesives. Despite decades of efforts on developing better wet adhesives, water and moisture still undermine strong adhesion to polar surfaces. Nature may, however, be able to point human beings in the right direction: marine mussels achieve durable underwater adhesion using a suite of proteins that are peculiar in having high levels of 3,4-dihydroxyphenylalanine (Dopa). The object of this research was to investigate the basic surface interactions employed by the mussels and roles of Dopa in mussel adhesion. I used the surface forces apparatus (SFA) and various other techniques to measure the interactions between mussel foot protein-3 *fast* (Mfp-3 *fast*) and the model substrate, mica, as well as the interactions between various Mfps.

Mussel adhesion is a complex biological system. To understand mussel adhesion, we have to understand the biophysics, chemistry, and biology involved in the mussel adhesive plaque. To translate our understanding of mussel adhesion further requires integrating established concepts from chemical engineering and materials science. This thesis is divided into four parts. The first two chapters introduce the basic knowledge and principles of mussel adhesion and intermolecular forces in biology. The third and fourth chapters describe the importance of interfacial redox to the adhesive properties of Mfp-3 *fast*. The adhesion of Mfp-3 *fast* to mica is closely coupled with Dopa redox and pH. During the formation of their adhesive plaques, mussels delicately control the redox environment of the plaques to achieve strong and stable adhesion. The fifth chapter shows the contribution of hydrophobic interactions to the Dopa-mediated adhesion/cohesion in mussel foot protein-3 *slow* (Mfp-3 *slow*). For practical adhesives, cohesion within the adhesive is as important as the interfacial adhesion. The hydrophobic interaction plays an important role in maintaining the structural integrity of mussel plaques. The last chapter presents a simple demonstration of how we can translate what we have learned from the mussel to making better wet adhesives by combining biology, biochemistry, and engineering. The simple peptide sequences

borrowed from mussel adhesive proteins could function as the basic building blocks for next generation wet adhesives.

I am deeply grateful to the following people who have read my thesis and made the publication of my thesis possible: Prof. Jacob Israelachvili, Prof. Herbert Waite, Nancy Emerson, and Abira Sengupta. Special thanks to my wife, Chen Chen, who has given great support to my life and research.

Pasadena, CA, USA Jing Yu

Acknowledgement

I must first thank my advisor Jacob Israelachvili for all his guidance and support over the past 5 years. He is truly exceptional as a scientist and as a person. The collaborative and supportive atmosphere in Jacob's group has always been the most beneficial factor in this long march, allowing me to grow and learn as a scientist and, more importantly, as a person. Working for Jacob has been a great pleasure and an honor.

Thanks should then go to Prof. Herbert Waite for his guidance and help during my Ph.D. I have benefited so much from his broad knowledge in biochemistry and, more generally, his attitude and dedication to science.

I must thank all the former and current members of the Israelachvili group. Nancy Emerson has been taking care of all my paper work, which makes my life so much easier. Kai Kristiansen has been there to free up seemingly endless seized screws, micrometers, and motors, as well as to make various new parts. Travers Anderson had much patience in teaching me how to use the SFA as well as the American culture such as baseball and football. Hongbo Zeng gave me a lot of help in my experiments. Xavier Banquy, Wren Greene, Steve Donaldson, Malte Hammer, Saurabh Das, Dongwoog Lee, Markus Valtiner, Matt Gebbie, and Mike Rapp have helped tremendously over the years—both from scientific and entertainment perspectives.

I must thank all my collaborators. Wei Wei has helped me so much in protein purifications and many biochemical tests. It has been a pleasure to work with her. Sathya Chery made all the structured surfaces for my gecko project. Professors Kimberly Turner, Michael Gordon, Joseph Zasadzinski, and Todd Squires have taken time out of their busy schedules to provide important insights and give much needed direction to my research.

I must thank my friends, Aviel Chaimovich and John Frostad, for their help over the past 5 years. Avi, you are a great roommate.

Finally I have to thank my family for their support. To my mother, I cannot thank you more. You have supported me every moment in my life. This Ph.D. is dedicated to you. To my wife, Chen, you are the greatest thing ever happened in my life! Your support is the most important thing to me in my life. I want you to know one thing: There is nothing ahead of you, not even research. Here comes the story you like.

The two-timing professor who comes home with clothes rumpled, hair disheveled, tie undone, and tiptoes into the bedroom. The light snaps on. “Explain yourself,” his wife demands. “Well,” he replies sheepishly, “I admire it. I was drinking with the boys and, well, I lost some money gambling, and there were women.” “You can’t fool me,” she says knowingly. “You’ve been doing research.”

About the Author

Jing Yu received his B.S. in Chemical Engineering from Tsinghua University, China, and obtained his Ph.D. in Chemical Engineering from University of California, Santa Barbara, in 2012, where he worked in Professor Jacob Israelachvili 's group. Dr. Yu grew up in Hangzhou, a beautiful city in eastern China. He received his B.Sc. in Chemical Engineering from Tsinghua University, China, and his Ph.D. in Chemical Engineering from University of California, Santa Barbara. Dr. Yu fell in love with the great sunshine and beach of the University of California, Santa Barbara campus during his 5 years Ph.D. where he worked in Professor Jacob Israelachvili's group. Yu conducted and pioneered outstanding research in many important areas including the wet adhesion of marine mussel adhesive proteins. Yu's work has been recognized by multiple international journals and online media sources including *Nature, Chemical Biology, ABC Science*, and the *Faculty of 1000*. Yu is currently a postdoctoral scholar in the Chemistry and Chemical Engineering Division at California Institute of Technology.

Contents

Chapter 1
Mussel Adhesion

1.1 Introduction

Nature has developed many fascinating species mastering in adhesion through the evolution of millions of years. Geckos have developed an extraordinary ability of climbing on vertical surfaces with various surface roughness and textures [1]. Similar abilities have also been observed on many insects such as fliers and ants [2]. Both geckos and insects apply hierarchical foot structures to maximize the real contact area and achieve reversible adhesion force via weak but universal van der Waals forces and sometimes capillary forces [2, 3]. The remarkable climbing ability of geckos and insects has inspired numerous studies on developing structured dry adhesives. On the other hand, many marine creatures use special adhesive proteins as super "glues" in ocean. Barnacles attach themselves permanently on various hard surfaces through adhesive plaques containing amyloid-like nanofibrils [4]. Sandcastle worms build their palaces by secreting special complex coacervate to glue together sand granules on the ocean floor [5]. Marine mussels are masters in wet adhesion, achieving strong and stable wet adhesion in the ocean through adhesive plaques mainly composed by various proteins [6]. The wet adhesion of barnacles, sandcastle worms, and mussels has been interesting to many scientists for the ability to overcome water and moisture, which are big enemies for many artificial adhesives.

1.2 Mussel Foot Proteins

Mussel adhesion is mediated by a holdfast structure known as the byssus, essentially a bundle of leathery threads tipped by flat adhesive plaques that attach to a variety of hard surfaces (Fig. 1.1). The other ends of the threads, the proximal ends, attach to the living tissues through the stem. The threads are made by the foot one at a time by an injection molding process followed by chemical cross-linking [7].

J. Yu, *Adhesive Interactions of Mussel Foot Proteins*, Springer Theses,
DOI 10.1007/978-3-319-06031-6_1,

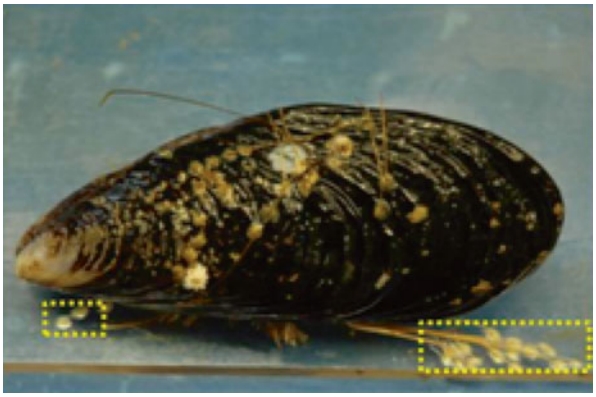

Fig. 1.1 A mussel (*M. californianus*) attaches to a polymer plate. The plaques are shown in *dotted yellow box*

Table 1.1 Biochemical comparison of the DOPA-containing proteins in the adhesive plaques and threads of Mytilus species

Protein	Mass (KDa)	pI	Dopa (mol%)	Repeating sequence	Location	References
Mfp-1	110	10	18	AKPSYPPTYK	Cuticle	[9, 12]
Mfp-2	45	10	5	EGF domain	Foam	[11]
Mfp-3	5–7	8–10	20	GYNG	Interface	[10]
Mfp-4	80	8.4	3	HVHRHRVLHG	Foam	[14]
Mfp-5	9	9.8	30	KY;YK	Interface	[13]
Mfp-6	11	9.3	4	None	Interface	[6]
pCOL-D	240	9.5	0.5	GlyXY, AH	Thr & plq	[16]
pCOLNG	240	8.8	0.5	GlyXY, AH	Thr & plq	[17]

At least eight proteins have been characterized from the adhesive plaques of Mytilus species, and several of them are well characterized (Table 1.1) [8–17]. Six important plaque proteins are named mussel foot protein (Mfp) through 1–6, all of which contain a posttranslationally modified amino acid 3,4-dihydroxyphenonyl-l-alanine (Dopa).

Mfp-1 is a crucial protein of the byssal cuticle. The Dopa groups in Mfp-1 form charge transfer complexes with Fe^{3+}. This charge transfer complex provides a mean of strong yet physical cross-linking and is responsible for the high hardness and high stiffness of the coating layer of the cuticle [18, 19]. Mfp-3 and Mfp-5 are the two major adhesive proteins in the plaque and have the highest Dopa content among all the Mfps [7, 20]. The high Dopa content gives both proteins strong adhesion on mineral surfaces, such as on mica and TiO_2 surfaces [8, 20, 21]. Although both proteins are major adhesive proteins in the plaque, they are quite different in terms of amino acid sequence, mass, and polymorphism. Mfp-3 is the most polymorphic protein among all the Mfps with more than 35 variants detected, whereas Mfp-5 is the

least polymorphic of all plaque proteins. Only two variants were discovered [7, 20]. The great variety of Mfp-3 suggests that the protein possibly plays multiple roles in the plaque, which will be further discussed in the following chapters.

The main theme of this work is exploring and understanding possible binding mechanisms of mussel proteins. Dopa is the prominent functionality in most Mfps that allows them to adhere to various surfaces underwater, as well as contributing to the cohesion within the plaques. Adhesive versatility is facilitated by Dopa's ability to form hydrogen bonds with hydrophilic surfaces (e.g., mica, hydroxyapatite) and participate in coordination bonding with metal ions and metal oxides and undermined by Dopa's notorious susceptibility to oxidation [8, 18, 21–23]. Various aspects related to the mussel protein adhesion and the interfacial redox of Dopa will be discussed in later chapters. In the following sections of this chapter, I will briefly review the rationales and goals of each subject studied and summarize the main conclusions.

1.3 Dopa Oxidation

Chapter 3 describes the effect of Dopa oxidation on the adhesion of Mfp-3 *fast*. The Dopa-containing proteins of mussels and sandcastle worms provide attractive design paradigms for engineering synthetic polymers for many applications as wet adhesives [7, 24–28], antifouling coatings [29, 30], magnetic imaging agents [31], tissue glues [32], and pH sensitive hydrogels [33]. Two major approaches have been applied by various groups to synthesize Dopa-/catechol-functionalized polymers: one is to graft Dopa or other catecholic groups to linear or branched poly(ethylene glycol) (PEG) by employing various ligation chemistries [34, 35]; the second approach is to copolymerize Dopa- or catechol-based monomers with other functional monomers by free radical polymerization [21]. Combined with different characterization methods, such as atomic force microscopy (AFM) and X-ray photoelectron spectroscopy (XPS), synthetic Dopa-modified polymers have provided some valuable insights of the binding mechanisms of Dopa to various surfaces [29, 36]. However, the effect of uncontrollable Dopa redox on the dependability of catechol as an anchoring functionality for polymers is a recognized problem in many applications and investigations mentioned above [21, 36]. A better understanding of interfacial Dopa chemistry is a crucial prerequisite to engineering the Dopa functionality for effective mussel-inspired polymer adhesion.

The aim of this study was to characterize and understand the role of Dopa in the adhesion of Mfp-3 *fast* and its related interfacial chemistry. As one key protein on the interface of the plaque, Mfp-3 *fast* functions as a biological glue, anchoring mussels on various surfaces. Mussels live in seawater with a pH of 8.2 and saturated with dissolved oxygen, under which Dopa can be readily oxidized to Dopaquinone. Given the vulnerable nature of Dopa, a general question rising up is that whether Dopa functions in its Dopa form in the mussel proteins.

To answer this question, I deposited thin films of Mfp-3 *fast* on mica and tested whether the adhesion and film thickness (hard wall) detected by the surface forces apparatus (SFA) is influenced by the presence or absence of Dopaquinone tautomers in the protein. Mfp-3 acted as an excellent wet adhesive on mica surface under low pH buffer conditions (pH-3), showing a strong adhesion energy of 2 mJ/m^2. Raising the pH of the solution to 7.5 completely abolished the bridging ability of Mfp-3 on the mica surface and significantly increased the thickness of the Mfp-3 films, indicated by the increase of the hard wall distance. Dopaquinones were formed in Mfp-3 by autoxidation (raising the pH) or by periodate-mediated oxidation. Further Dopaquinone tautomerization was evident by UV–Vis spectrophotometry (UV–Vis) and circular dichroism (CD) spectroscopy measurements, suggesting that a tautomer of Dopaquinone, α,β-dehydrodopa, is responsible for the size increase of Mfp-3 fast molecules.

The experimental results led to a deeper understanding of the role of Dopa and interfacial Dopa chemistry in the adhesion of mussel proteins. The necessity of Dopa in its reduced form in maintaining strong adhesion of Mfp-3 *fast* demonstrates that Dopa is the crucial anchoring group for Mfps. Protein Dopaquinone tautomerization is intriguing because of its effect on the α,β-carbons in the peptide backbone and the suggestion that the backbone flexibility of adhesive proteins may be adjusted by the selection of different resonance forms of Dopa following oxidation. This runs against the conventional wisdom that oxidation of Dopa-containing proteins serves exclusively as a cross-linking strategy. A spatially tuned control of α,β-dehydrodopa formation would enable an extraordinary versatility in how the proteins are packed as they approach a solid surface, which could be responsible for the obvious porosity gradient in the plaque.

1.4 Interfacial Redox in the Mussel Plaque

Chapter 4 describes the interfacial redox in the mussel plaque. Chapter 3 already elaborated that the importance of Dopa in the underwater adhesion of marine mussels, and the susceptibility of Dopa to oxidation, often renders it unreliable for adhesion and limits the application of Dopa-functionalized synthetic polymers as adhesives and coating materials [36, 37]. To perform both functions, the polymers have to intact strongly with one or both substrate surfaces, which requires Dopa staying in its reduced form on many inorganic and metal oxide surfaces [38]. This unreliability also raises the question why mussels chose to rely on the Dopa proteins for adhesion despite of the easy surrender of Dopa to oxidation. The answer of this question has considerable biological and technological value.

In the mussel plaque, Dopa functions not only in its reduced form but also in its oxidized form: oxidation-induced Dopa cross-linking plays an essential role in the cohesive strength of the plaque [7, 39, 40]. To achieve both strong adhesion and cohesion requires a careful control of the two redox states of Dopa, both temporally

and spatially, as demonstrated by mussels. The ability to precisely control the redox state of Dopa is also of great benefit to many biomedical applications such as dental or bone glues, which usually require both strong adhesion (at the interface) and cohesion (in the glue).

The aim of this study was to investigate how mussels control the redox state of Dopa in plaques. Despite of the vulnerable nature of Dopa under seawater conditions, mussels seem to achieve a perfect control over the interfacial redox of Dopa in their byssal attachment plaques. Exploring the redox chemistry in the mussel plaques can deepen our understanding on the mussel adhesion, as well as can guide people designing better synthetic Dopa-functionalized polymers for many engineering applications.

The secretion of adhesive proteins was induced by injecting potassium chloride, and the pH in the distal depression was monitored by a microelectrode. Just prior to the secretion of plaque proteins, the pH of the distal depression dropped from a resting pH of 7.3–5.8 within 2 min of induction, suggesting that mussels limit Dopa oxidation by imposing an acidic, reducing regime in the confined space of Mfps deposition. MALDI TOF mass spectrometry showed that, after induced protein secretion, mussels first secreted Mfp-3 on the substrate followed by Mfp-6, a cysteine-rich protein, in less than 1 min. The high cysteine/thiol content in Mfp-6 suggests that it is a redox sensitive protein and may play a key role in the redox balance of the plaque.

Using the SFA technique, I demonstrated that the adhesion of Mfp-3 to mica is closely coupled with Dopa redox and pH. Raising the pH from 3 to 7.5 decreased the adhesion energy of Mfp-3 on mica 20-fold and appeared to be driven by the pH-dependent oxidation of Dopa. Addition of thiol-rich Mfp-6 restored Mfp-3 adhesion by coupling the oxidation of thiols to the reduction of Dopaquinones. To confirm this redox effect of Dopa in mussel adhesion, an artificial oxidant, sodium periodate ($NaIO_4$), was added into the gap of two films of Mfp-3 fast at pH 3 to oxidize the Dopa group and titrate the adhesion of Mfp-3 fast. A correlation between the amount of periodate added into the gap and the decrease of adhesion was observed. With regard to antioxidants, ascorbic acid was applied to reduce Dopaquinone in oxidized Mfp-3 and in doing so rescued a substantial proportion of adhesion. The consistence between the loss of adhesion by autoxidation at pH 7.5 or periodate oxidation and the rescuing of adhesion by adding antioxidants, either thiol-rich Mfp-6 or ascorbic acid, supports the hypothesis that mussels control the local redox environment of the plaque to prevent Dopa oxidation.

1.5 Cohesive Proteins in the Mussel Plaque

In Chap. 5, I describe one possible strategy that mussels take to achieve the mechanical strength of their plaques. Mussel byssal plaques have amazingly complicated hierarchical architectures, which consist of bundles of microfibers separated by a

granular matrix, a porous plaque core with a gradient of pore sizes from the top to bottom of the plaque, and a hard but extensible cuticle coating layer [7]. This amazingly well-organized structure is constructed by 8–9 proteins in the plaque [7, 8, 41].

Various intermolecular interactions are employed by the proteins to fulfill various functions. Adhesive proteins Mfp-3 *fast* and Mfp-5 locate at the front line of the plaque and act like "super glues," providing strong adhesion on various substrates [8, 20, 23]. Mfp-6, a thiol-rich natural antioxidant, manipulates the interfacial redox of the Dopa in the plaque, preserving the adhesion power of Dopa during the formation of the plaque and later contributing to the cohesive strength of the plaque by covalently cross-linking with Dopaquinone [6, 15, 22]. The Dopa side chains in the protective protein, Mfp-1, can complex with Fe^{3+}, offering both high hardness and high toughness to the cuticle coating layer [19, 21]. Recent SFA tests also suggest other types of metal bridging, including Ca^{2+} and Mg^{2+} ion binding, contributing to the protein–protein binding complex in the plaque [41]. Understanding various interactions involved in the adhesion and cohesion of the mussel plaque can help us better understand the structure–properties relationship of the mussel plaque. This sizing up biology also has profound impacts on bottom-up designs of better engineering adhesives.

The primary aim of this research was to investigate the possible roles of Mfp-3 in the mussel byssal thread. Dopa-rich Mfp-3 has about 30 different variants in the mussel plaque, which can be subdivided into two groups, Mfp-3 *fast* and *slow*, due to the posttranslational modification of protein tyrosine and arginine to Dopa and 4-hydroxyarginine [6]. In previous studies, focus had been on the adhesion properties and performance of Mfp-3 *fast*, which was shown to be able to bridge two mica surfaces. The other big family of the Mfp-3 variants, Mfp-3 *slow*, is less well understood. The hydrophobic interaction, a long-range interaction, is significant to protein function in terms of driving protein folding and self-assembly in biomacromolecules. The lower charge density results in Mfp-3 *slow* being a very hydrophobic protein, suggesting the hydrophobic interaction may possibly play a major role in the mussel plaque. Given the abundance of Mfp-3 *slow* in the mussel plaque, a close investigation of the function of this protein and the possible involvement of the hydrophobic interaction were highly desired.

Using an SFA to investigate the adhesion of Mfp-3, I have discovered a subtle molecular strategy apparently based on hydrophobicity for tuning adhesion despite Dopa's instability. In contrast to other adhesive proteins, (1) the adhesion energy of Mfp-3 *slow* on mica surfaces at pH 3 is about half that of Mfp-3 *fast* and roughly proportional to its lower Dopa content. The trend of decreasing adhesion with increasing pH is significantly less pronounced than what was reported for Mfp-3 *fast*; (2) there exists a reversibly strong cohesive interaction of about $E_{ad} = -3$ mJ/m^2 between two Mfp-3 *slow* protein films over a wide range of pH (from 3 to 7.5). This cohesion probably reflects the cumulative effects of Dopa-mediated hydrogen bonding, other inter-residue hydrogen bonding, and especially hydrophobic interactions since Mfp-3 *slow* is the most hydrophobic of mussel adhesive proteins. Exploitation of hydrophobic sequences to protect Dopa against oxidation as well as

incorporating hydrophobic interactions and inter-residue H-bonding to strengthen adhesives expands our understanding of biological wet adhesion and also provides new perspectives for developing effective artificial underwater adhesives.

1.6 Biomimetic Adhesive Peptides

Chapter 6 describes the binding mechanism of three mussel-inspired synthetic peptides to the mica surface. All three peptides were derived from the amino acid sequence of the molecular superglue, Mfp-5. Of all the known Mfps, Mfp-5 holds the crown of having the highest Dopa content and exhibits the strongest adhesion energy on mica substrates [20]. Given these distinctions, Mfp-5 has become an attractive molecular paradigm for mimicking mussel adhesion and has inspired numerous investigations of Dopa- or catechol-functionalized synthetic materials for various applications [7, 25, 27–30, 33]. In previous chapters I have emphasized the importance of Dopa in mussel protein adhesion. However, due to the large size and complexity of the Mfps molecules, significant details of the protein binding mechanism remain unclear [20, 22, 23]. Two persistent questions are as follows: (1) How do the flanking amino acid sequences affect Dopa adhesion? (2) How do interactions besides those involving Dopa help to mediate the adhesion of Mfps [42]?

The answer to the first question is highly desired since various reports have shown that Dopa-functionalized synthetic polymers cannot perform at the same level of Mfps [21, 29], indicating mussels may have developed some synergistic strategies, possibly by incorporating various amino acids with Dopa in the protein sequences, to optimize the adhesion of Mfps. Given that nature has optimized mussel proteins for adhesion over millions of years, these synergistic effects should not be so surprising. The second question arises from various SFA studies on Mfp-3 fast and Mfp-5. Both proteins have isoelectric points (pIs) around ten and are highly positively charged at the pH of seawater. At pH 7.5, strong attractive electrostatic interactions should be expected by the positively charged proteins and negatively charged mica surfaces. Such interactions, however, have not been observed by previous SFA measurements, possibly because of the high ionic strength of the buffer (~0.3 M) and the steric repulsions due to the large sizes and complexities of the proteins [43].

To answer these questions, three short, Mfp-5-derived synthetic peptides 15–16 residues in length were prepared with and without enzymatic modification of tyrosine (Y* denotes tyr to Dopa): VGSGY*DGY*SDGY*Y*DG (PEP pI 4), HY*HSGGSY*HGSGY*HG (PEP pI 6.5), and GY*KGKY*Y*GKGKKY*Y*Y*K (PEP pI 10) [44]. The repulsive and attractive forces of these peptides on mica surfaces were investigated with an SFA. All three Mfp-5-derived peptides showed adhesion energies that are at least an order of magnitude lower than that of intact Mfp-5, suggesting that there are synergistic effects from the amino acid residues across the whole protein sequence, which cannot be achieved by protein fragments. Increasing pH significantly reduces the adhesion energies of three peptides due to both Dopa oxidation and the change of both the magnitude and signs of charges on

the three peptides. Further evidences of the involvement of electrostatic interactions were provided by periodate oxidation control experiment with changing the solution pH; significant differences in the adhesion energies of three peptides on mica were observed when oxidizing Dopa by autoxidation at pH 7.5 or periodate oxidation.

1.7 Organization of This Dissertation

Chapter 2 starts with a brief description of some important surface interactions relevant to this work, followed by a short description of the SFA technique. Chapter 3 describes with the effect of interfacial redox on Mfp-3 adhesion, which demonstrates how Dopa oxidation can lead to a loss of adhesion of Mfp-3 on the mica surface. Chapter 4 further explores the importance of interfacial redox in mussel adhesion and describes two strategies that mussels take to control the interfacial redox and Dopa adhesion: controlling the local pH of the plaque and adding antioxidants. Chapter 5 describes the cohesive interaction of Mfp-3 *slow*. Hydrophobic interactions play a crucial role in the system. Finally, Chap. 6 shows an example of designing mussel-inspired peptide adhesives and demonstrates that the peptides adhere to the mica surface via multiple binding mechanisms.

References

1. Autumn K et al (2000) Nature 405(6787):681–685
2. Bullock JMR, Federle W (2011) Naturwissenschaften 98(5):381–387
3. Autumn K et al (2002) Proc Natl Acad Sci U S A 99(19):12252–12256
4. Barlow DE et al (2010) Langmuir 26(9):6549–6556
5. Zhao H et al (2005) J Biol Chem 280(52):42938–42944
6. Zhao H et al (2006) J Biol Chem 281(16):11090–11096
7. Lee BP et al. (2011) Ann Rev Mater Res 41:99–132
8. Lin Q et al (2007) Proc Natl Acad Sci U S A 104(10):3782–3786
9. Deacon MP et al (1998) Biochemistry 37(40):14108–14112
10. Papov VV et al (1995) J Biol Chem 270(34):20183–20192
11. Rzepecki LM, Hansen KM, Waite JH (1992) Biol Bull 183(1):123–137
12. Waite JH, Housley TJ, Tanzer ML (1985) Biochemistry 24(19):5010–5014
13. Waite JH, Qin XX (2001) Biochemistry 40(9):2887–2893
14. Zhao H, Waite JH (2006) Biochemistry 45(47):14223–14231
15. Zhao H, Waite JH (2006) J Biol Chem 281(36):26150–26158
16. Qin XX, Coyne KJ, Waite JH (1997) J Biol Chem 272(51):32623–32627
17. Waite JH, Qin XX, Coyne KJ (1998) Matrix Biol 17(2):93–106
18. Harrington MJ et al (2010) Science 328(5975):216–220
19. Zeng HB et al (2010) Proc Natl Acad Sci U S A 107(29):12850–12853
20. Danner EW et al (2012) Biochemistry 51(33):6511–6518
21. Anderson TH et al (2010) Adv Funct Mater 20(23):4196–4205
22. Yu J et al (2011) Nat Chem Biol 7(9):588–590
23. Yu J et al (2011) Adv Mater 23(20):2362–2366
24. Wang JJ et al (2008) Adv Mater 20(20):3872–3876

25. Park KM, Park KD (2011) J Mater Chem 21(40):15906–15908
26. Ceylan H et al (2012) Soft Matter 8(14):3929–3937
27. Shafiq Z et al (2012) Angew Chem Int Ed 51(18):4332–4335
28. You I et al (2012) Angew Chem Int Ed 51(25):6126–6130
29. Dalsin JL et al (2003) J Am Chem Soc 125(14):4253–4258
30. Kuang JH, Messersmith PB (2012) Langmuir 28(18):7258–7266
31. Lee YH et al (2008) Adv Mater 20(21):4154–4157
32. Brubaker CE, Messersmith PB (2011) Biomacromolecules 12(12):4326–4334
33. Holten-Andersen N et al (2011) Proc Natl Acad Sci U S A 108(7):2651–2655
34. Lee BP, Dalsin JL, Messersmith PB (2002) Biomacromolecules 3(5):1038–1047
35. Brubaker CE et al (2010) Biomaterials 31(3):420–427
36. Lee H, Scherer NF, Messersmith PB (2006) Proc Natl Acad Sci U S A 103(35):12999–13003
37. Proudfoot GM, Ritchie IM (1983) Aust J Chem 36(5):885–894
38. Nicklisch SCT, Waite JH (2012) Biofouling 28(8):865–877
39. Rzepecki LM, Nagafuchi T, Waite JH (1991) Arch Biochem Biophys 285(1):17–26
40. Liu B, Burdine L, Kodadek T (2006) J Am Chem Soc 128(47):15228–15235
41. Hwang DS et al (2010) J Biol Chem 285(33):25850–25858
42. Krivosheeva O, Dedinaite A, Claesson PM (2012) J Colloid Interface Sci 379:107–113
43. Israelachvili JN (2011) Intermolecular and surface forces, 3rd edn. Academic, Burlington, MA
44. Taylor SW (2002) Anal Biochem 302(1):70–74

Chapter 2
Surface Interactions in Biological Systems

2.1 Overview of Intermolecular Interactions in Biological Systems

Intermolecular interactions are the attractive or repulsive interactions existing between molecules in a substrate. There are a number of seemingly different categories, but all of them originate from one fundamental force—the electromagnetic force [1]. The development of quantum theory greatly deepens our understanding on the nature of intermolecular interactions. Theoretically, all the intermolecular interactions can be calculated using the quantum theory; however, due to the extreme difficulty of solving the exact or even approximate solutions of the Schrödinger equation, the historical way of dividing the intermolecular interactions into several categories with each of them having a simple interaction potential is still the most effective and dominating approach. Assuming the pair potential between two atoms or molecules are additive, integrating the potentials over all the atoms or molecules in the substrates gives the interfacial interactions. While the origins of the additive interactions are similar to those of the intermolecular interactions, they can quite often exhibit new features when acting between two macroscopic bodies. Strictly, the words "force" and "interaction" have different meanings, but for the convenience of the author, here I clarify the two words "force" and "interaction" will be used interchangeably in this dissertation when referring to surface interactions. The force is simply the derivative of the interaction potential, $F = -dW/dD$, and both of them are functions of distance D.

Due to the complexity of the biological systems, intermolecular interactions involved in biological systems are quite complex and dynamic [2]. The types of interactions involved in biological molecules, however, are no different from those involved in any other systems (Fig. 2.1). Dealing with protein–substrate and protein–protein interactions, some basic surface interactions are fundamental to this dissertation and, therefore, a brief description of them, including the van der Waals (VDW) forces, electrostatic forces, steric (polymer-mediated) forces, and special interactions such as hydrogen bonding and hydrophobic forces, will be included in this chapter.

J. Yu, *Adhesive Interactions of Mussel Foot Proteins*, Springer Theses,
DOI 10.1007/978-3-319-06031-6_2,

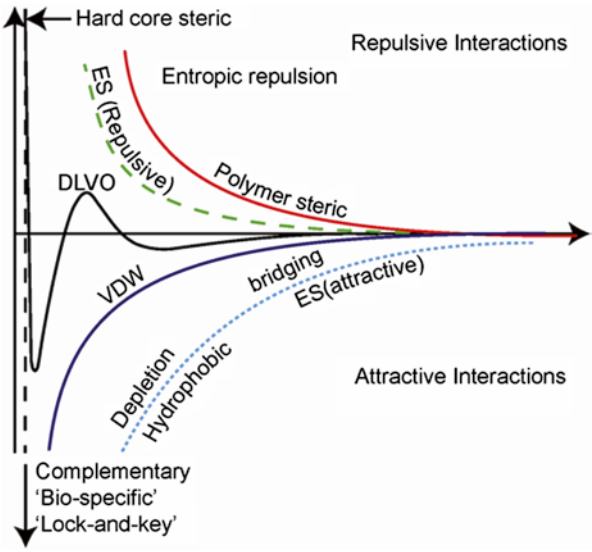

Fig. 2.1 Illustration of some common interactions in aqueous solutions. Figure adopted from Leckband and Israelachvili [2]

2.1.1 van der Waals (VDW) Forces

The VDW forces, or the dispersion forces, are a type of universal forces that act between all atoms and molecules, thus playing a major role in a number of important phenomena such as adhesion, wetting, surface tension, the properties of gas and lipids, and the structure of condensed macromolecules. For polar molecules, the VDW forces contain three different types of forces: the induction force, the orientation force, and the dispersion force; whereas for nonpolar, only the third type of force, the dispersion force, contributes to the VDW forces. The dispersion forces present between all the atoms and molecules and, therefore, are probably the most important component to the VDW forces. The dispersion forces are long ranged and can be repulsive or attractive, depending on the types of molecules and the presence of neighboring molecules. The forces are quantum mechanical in origin, and a rigorous treatment requires using quantum electrodynamics, but the nature of the dispersion forces can be understood intuitively by considering a simple model of two nonpolar atoms (such as helium atoms) interacting in vacuum. For each helium atom, the time-averaged dipole moment is zero; however, at any given instant, there is a finite dipole moment due to the fluctuation of the electron clouds in relation to the nucleus. This instantaneous dipole moment creates an electric field which acts on the nearby helium atom and introduces an instantaneous dipole moment in it. The two dipole moments give rise to an instantaneous attractive interaction between two atoms that has a finite value when time averaged. For simplicity, the interaction potential of the VDW forces between two atoms can be expressed as

$$w(r) = -\frac{C_{\mathrm{VDW}}}{r^6} \tag{2.1}$$

where C_{VDW} is a constant depending on the type of molecules [1].

Assuming a simple pairwise additivity (which is not always true), one can integrate the interaction potentials of all the atoms in two bodies to get the interaction potential for two surfaces with different geometries in terms of the *Hamaker* constant

$$A = \pi^2 C_{\mathrm{VDW}} \rho_1 \rho_2 \tag{2.2}$$

where ρ_1 and ρ_2 are the number of atoms or molecules per unit volume in the two bodies [1].

A more rigorous calculation of the *Hamaker* constant can be obtained though the *Lifshitz theory* [1]. Here I just introduce an approximate expression for the nonretarded *Hamaker* constant for two media 1 and 2 across a third medium 3:

$$A_{\mathbf{total}} = A_{v=0} + A_{v>0} \approx \frac{3}{4} kT \left(\frac{\varepsilon_1 - \varepsilon_3}{\varepsilon_1 + \varepsilon_3} \right) \left(\frac{\varepsilon_2 - \varepsilon_3}{\varepsilon_2 + \varepsilon_3} \right) + \frac{3h\nu_e}{8\sqrt{2}} \frac{\left(n_1^2 - n_3^2 \right)\left(n_2^2 - n_3^2 \right)}{\left(n_1^2 + n_3^2 \right)^{1/2} \left(n_2^2 + n_3^2 \right)^{1/2} \left\{ \left(\left(n_1^2 - n_3^2 \right) + \left(n_2^2 - n_3^2 \right) \right) \right\}}, \tag{2.3}$$

where ε_1, ε_2, and ε_3 are the dielectric constants for media 1, 2, and 3 and n_1, n_2, and n_3 are the refractive indexes for media 1, 2, and 3, respectively [1].

2.1.2 Electrostatic Interactions

The electrostatic Coulomb forces between two charged atoms or ions are the strongest physical forces. The free energy between two charges Q_1 and Q_2 is given by the simple Coulomb Law:

$$W(r) = \frac{Q_1 Q_2}{4\pi\varepsilon_0 \varepsilon r}, \tag{2.4}$$

where ε_0 is the permittivity of free space. Coulomb force has a distance dependence of only $1/r$; therefore it decays slowly with the distance and is strong and long range [1]. Like the VDW forces, the electrostatic static interactions between charged surfaces in a solution (usually water for biological systems) are more complicated and more interesting.

The long-ranged electrostatic interactions play important roles in many biological processes. Many biological molecules and surfaces are charged due to the ionization/dissociation of surface groups or the adsorption of ions from solution onto an uncharged surface/molecules. The surface charge is balanced by counterions in solution, distributed in a tightly bounded stern layer (or Helmholtz layer) and a diffuse electric double layer. The "thickness" of this layer can be described by the Debye length, $1/\kappa$. κ is defined as

$$\kappa = \left(\sum_i \rho_{i\infty} e^2 Z_i^2 / \varepsilon_0 \varepsilon kT \right)^{1/2} \mathrm{m}^{-1}, \tag{2.5}$$

where $\rho_{i\infty}$ is the number density of ions of valency z_i in the bulk solution [1]. In biological systems, due to the high ionic strength of the body fluid, this Debye length is usually small (less than 1 nm).

Theoretically the electrostatic interaction between two surfaces or two bodies can be obtained by solving the Poisson Boltzmann (PB) equation:

$$\frac{d^2\psi}{dx^2} = \frac{-ze\rho}{\varepsilon_0\varepsilon} = \frac{-ze\rho_0}{\varepsilon_0\varepsilon} e^{-ze\psi/kT}, \tag{2.6}$$

where ψ is the electrostatic potential [1]. Applying various boundary conditions which correspond to different physical conditions, solutions for the PB equation can be taken out, although usually with great challenges due to the nonlinearity of this second-order differential equation.

In solutions, the total interaction between two charged surfaces must include both the VDW interactions and electrostatic interactions. Those two interactions form the basis of the landmark Derjaguin-Landau-Verwey-Overbeek theory [3, 4], which has been widely applied in explaining the interactions between colloidal particles and membrane surfaces [5, 6].

2.1.3 *Polymer-Mediated Interactions: Steric Repulsion and Bridging Adhesion*

(1) *Steric Repulsion*

Polymers can adsorb on surfaces either through physical interactions (physisorption) or via chemical reactions (chemisorption). Depending on the interactions between the polymers and surfaces, the grafting density, and the solvent conditions, the adsorbed polymers can exhibit different states on a surface: they can stay the same as their coiled state in solution, such as the mushroom state, or they can form a surface-induced structure, for instance, a brush layer. When the adsorbed polymer layer approaches another surface, it experiences a repulsive osmotic force due to the loss of entropy caused by compressing the polymer chains between two surfaces. This entropic repulsion is usually referred to as the steric repulsion [1, 2].

The actual range and magnitude of the steric repulsion depend on the type of polymers, the molecular weight of the polymer chains, graft density, solution conditions, temperature, and the interactions between the polymer chains and surfaces. The steric repulsion typically starts no further than the contour length L of the polymer chains ($2L$ if both surfaces are coated by polymers) and grows exponentially over a range of distance, till the distance reaches a few times of the radius of gyration of the polymer chains, R_g, beyond which the repulsion becomes much steeper as the polymer chains become increasingly compacted.

(2) *Attractive Intersegment and Bridging Forces*
In a poor solvent, segments of polymers attract each other due to VDW, hydrophobic, electrostatic, and H-bonding interactions. This attractive intersegment interaction is extremely important in biology, giving rise to the secondary structures of proteins and the double helical structure of DNA, perhaps two most important structures for all the lives on earth [1, 2]. Similarly, when two polymer-coated or protein-coated surfaces come together in a poor solvent, the intersegment attraction between polymer or protein chains gives rise to an attractive interaction between two surfaces [1]. If two surfaces are further compressed, the steric interaction eventually wins out and the overall interaction becomes repulsive. But an adhesion force can be measured during the separation of two surfaces. I will come back to this scenario in Chap. 5.

Another important polymer-mediated attraction is the so-called bridging forces. According to the origin of the adhesion, the bridging forces can be divided into two groups: specific and nonspecific. The former involves specific interactions or chemical reactions and commonly exists in biological system, whereas the latter exists mostly in nonbiological systems. Specific bridging adhesion is a centerpiece of this dissertation, thanks to the bidentate H-bonding nature of Dopa-mediated adhesion on the mica surface.

2.1.4 Water-Mediated Interactions: The Hydrogen Bond and the Hydrophobic Interaction

(1) *Hydrogen Bond*
Water is unique, not only because it is the solvent for life, but also because the anomalous properties and special interactions associated to water: the hydrogen bond and the hydrophobic interaction.

The hydrogen bond is responsible for most of water's unique properties: the unusually high melting and boiling temperatures, the density maximum at 4 °C, and the less density of solid ice in comparison to liquid water. Hydrogen bonds are also very important for the structure of many biological macromolecules, helping stabilize the double helical structure of DNA and the secondary structures of proteins, such as the α-helix and the β sheets [1]. Like many other proteins, mussel adhesive proteins also utilize hydrogen bonds: Dopa is capable of forming a bidentate hydrogen binding (two hydrogen bonds) to many mineral surfaces, including mica [7, 8].

The hydrogen bond is mostly electrostatic in nature, but it shears some features of covalent bonds, such as high single bond strength and fairly directional. Both features are important to the binding of Dopa to the mica surface. The surprising matching between the distance of two hydroxyl groups of Dopa and the lattice structure of mica makes it possible for Dopa to form a bidentate hydrogen binding to the mica surface, giving rise to the strong adhesion force between different Mfps and the mica surface [7]. More details will be covered in Chap. 3.

(2) *Hydrophobic Interaction*

The second important water-mediated interaction, the hydrophobic interaction, is related to the H-bonding network of water molecules and the resulting tetrahedral structure of water [1]. When water molecules interact with nonpolar molecules (such as hydrocarbons) that are incapable of forming hydrogen bonds with water molecules, they lose the ability of maintaining their normal H-bonding network. Water solves this problem by two ways, which give the two limits of the hydrophobic interactions. When the nonpolar solute molecule is small (the diameter is typically smaller than 1 nm), water molecules can rearrange themselves around it without breaking their H-bonding network. Although its rearrangement requires an entropy penalty, it is energetically favorable [9]. The other extreme happens when water molecules are facing a big hydrophobic surface or subject, on which water molecules cannot maintain the tetrahedral H-bonding network. How water molecules deal with this situation is still not clear and is a very hot research topic [10]. Some computer simulations suggest that under such conditions, hydrophobic surfaces create excluded volume regions where the density of water molecules vanishes [11], whereas others suggest the hydrophobic surface does not create excluded volume, instead, it increases the fluctuations of the density of water molecules near the surface [10, 12]. Despite numerous efforts on trying to uncover the nature of the hydrophobic interaction, no satisfactory theory yet has been established. I am hoping this situation will be reversed in the next decade, thanks to the brilliant minds that devote their careers to studying this mysterious but extremely important interaction.

The hydrophobic interaction is certainly one of the most important interactions for life, if not the most important interaction [13]. It holds the membrane together for cells, directly guides the self-assembly of proteins, and is responsible for the stability of the double helical structure of DNA [1]. It also plays a key role in maintaining the mechanical strength of the mussel plaque, as I will describe in details in Chap. 5.

2.2 Adhesion

2.2.1 Surface Energy, Interfacial Energy, and Work of Adhesion/Cohesion

The free energy changes to separate two surfaces or media from contact to infinity in a vacuum is called the work of adhesion W_{12} (for two different media) or the work of cohesion W_{11} (for two identical media) [1].

Surface energy γ is the free energy change when the surface area of a medium is increased by unit area. The surface energy is related to the work of cohesion W_{11} by a simple relation of

$$\gamma_1 = \frac{1}{2} W_{11}. \tag{2.7}$$

The interfacial energy γ_{12} is the free energy change in expanding the interface area of two immiscible liquids 1 and 2 or one solid 1 and one liquid 2 by unit area. The work of adhesion and the interfacial energy are related through the Dupoé equation:

$$W_{12} = \gamma_1 + \gamma_2 - \gamma_{12} \tag{2.8}$$

A similar equation can be derived for separating two dissimilar media 1 and 2 in medium 3:

$$W_{132} = \gamma_{13} + \gamma_{23} - \gamma_{12}. \tag{2.9}$$

2.2.2 Adhesion Energies and Adhesion Forces

Although sometimes used interchangeably, we have to notice that the adhesion energy and the adhesion force are two different things. Strictly, the adhesion energy is an equilibrium term, and it should only depend on the initial and final states. To measure it accurately, the measurement has to be infinitely slow or, in other words, in a reversible process. Adhesion force, on the other hand, is a dynamic term and usually depends on the pathway through which the measurement is preformed (e.g., pulling off a tape as a whole requires a much larger force in comparison to peeling off the tape from one side), the experimental geometry, and the rate at which the measurement is performed. For example, when nonequilibrium and rate-dependent interactions are involved, very different forces can be measured depending on the rates at which the surfaces are separated, though the net energy change is the same [1]. This problem is also encountered in our surface forces apparatus (SFA) measurement. Here I clarify that I will use the terms "adhesion energy" and "work of adhesion" throughout this dissertation, but the "adhesion energies" I report here are not the equilibrium values. Depending on various interactions involved and different natures of different proteins, some values are close to the equilibrium values, while others may be off by quite a bit.

2.3 Surface Forces Apparatus

The main technique I have used in my research is the SFA. The SFA is a powerful instrument to measure forces between surfaces. It was first developed in the 1960s and then modified by Israelachvili et al. in the 1970s to measure the VDW forces in air down to a few nanometers [14]. Since then, the SFA technique has been continuously modified [15, 16]. The ability to measure forces in various liquids greatly extended the territory of the SFA, allowing it to measure almost all the surface forces: the VDW, electrostatic, DLVO, hydrophobic, hydration, and polymer-mediated steric forces [5, 14–16]. Starting in the 1990s, the SFA technique has been applied to measure the interactions in complex biological systems involving membranes and membrane proteins [17–19].

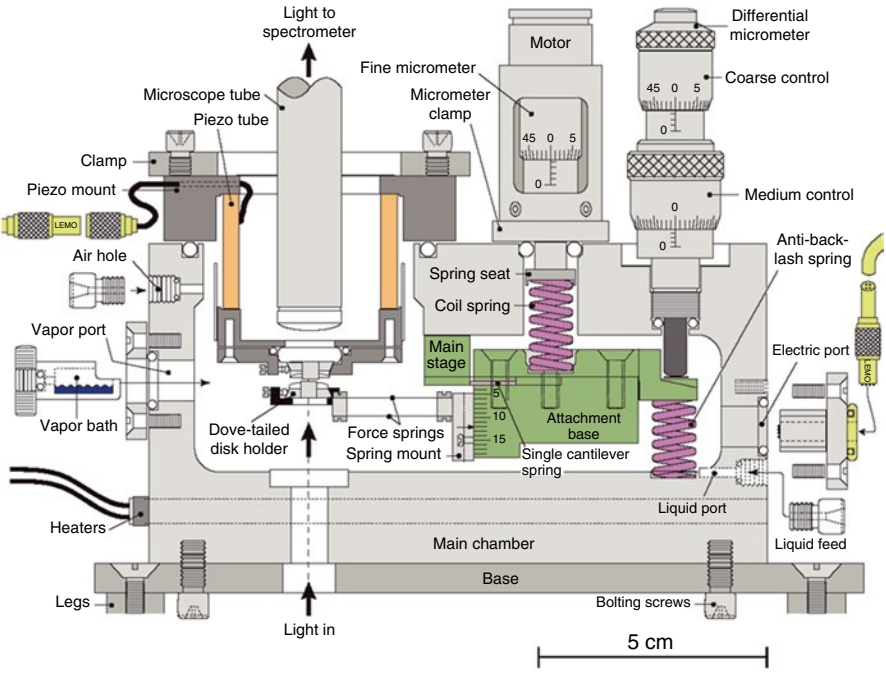

Fig. 2.2 A schematic diagram of the SFA 2000

2.3.1 SFA 2000

The most recent model of SFA, the SFA 2000, is shown in Fig. 2.2 [20]. An important feature of an SFA is its ability to control the distance between two surfaces through four different controls, from a coarse control of a micrometer, which can move the surfaces by millimeters, to an extra fine control of a piezoelectric tube, which allows for a sub-nanometer control for the distance between the surfaces. In a basic SFA setup, the upper surface is mounted to a piezoelectric tube, and the bottom surface is mounted to a force measuring double cantilever spring. Upon deflection, the double cantilever spring bends normally to the upper surface, which also gives the normal forces according to Hooke's Law, $F = K\Delta x$, where K is the spring constant and Δx is the deflection of the spring.

2.3.2 Multiple Beam Interferometry

The distance between the surfaces and the shape of the surface are measured in the SFA using the method of multiple beam interferometry (MBI) [14]. For an accurate distance resolution, the MBI technique requires very smooth and highly reflective

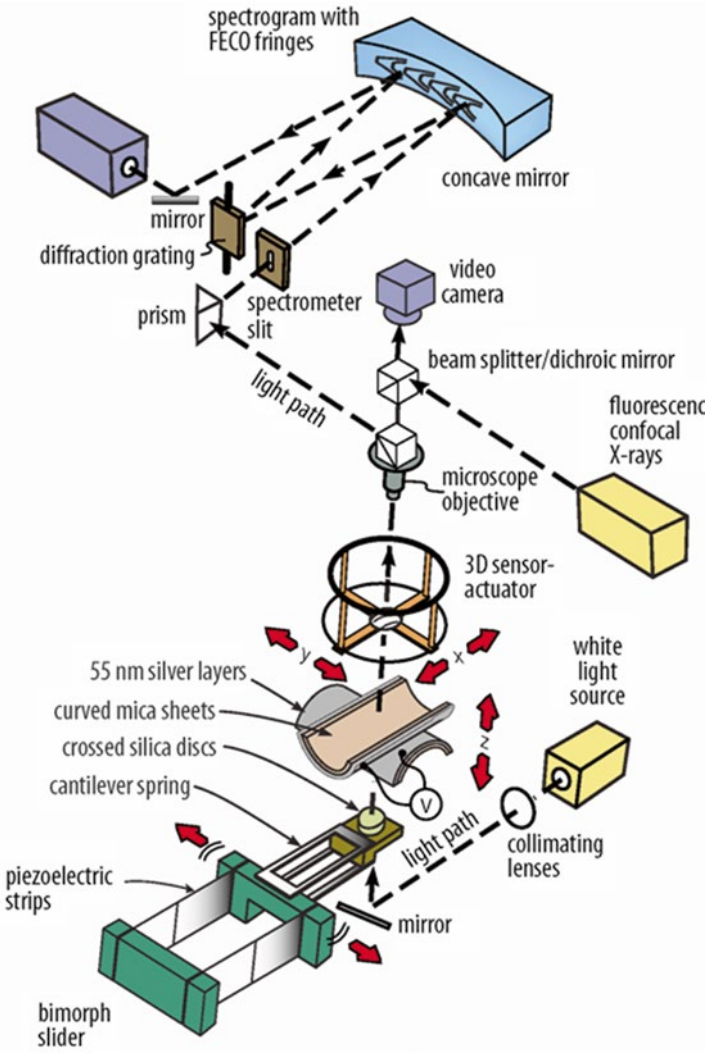

Fig. 2.3 Schematic of the multiple beam interferometry technique in the SFA

surfaces. In a typically SFA experiment (Fig. 2.3), a pair of freshly cleaved, uniformly thick, thin (usually 2–5 μm) mica surfaces are used as the surface substrate. The mica is coated with a thin (~55 nm) silver film on the back for providing a good interfering pattern between the reflecting surfaces. The surfaces are then glued on two cylindrical-shaped silica disks and mounted in the SFA with a cross-cylinder geometry, which is equivalent to a sphere on a flat surface geometrically.

White light is guided to the surface, but due to the constructive interference of the light within the silver mirrors, only discrete wavelengths λ_n^0 ($n=1,2,3,\ldots$) can pass though the surfaces, creating interference fringes known as fringes of equal chromatic

order (FECO), which can be separated by a spectrometer and recorded by a video camera. The order of the fringe, *n*, is equal to the number of antinodes in the electromagnetic standing wave between two mirrors. Since mica is birefringent, FECO fringes appear as doublets with the β and γ components. For a mica-medium-mica geometry, the distance between the surfaces can be determined by a master equation:

$$\tan\left(\frac{2\pi\mu D}{\lambda_n^D}\right)=\frac{2\bar{\mu}\sin\left(\dfrac{1-\lambda_n^0/\lambda_n^D}{1-\lambda_n^0/\lambda_{n-1}^0}\pi\right)}{\left(1+\bar{\mu}^2\right)\cos\left(\dfrac{1-\lambda_n^0/\lambda_n^D}{1-\lambda_n^0/\lambda_{n-1}^0}\pi\right)\pm\left(\bar{\mu}^2-1\right)}, \tag{2.10}$$

where μ is the refractive index of the medium, $\bar{\mu}=\mu_{\text{mica}}/\mu$ is the effective refractive index, and ± refers to odd and even order fringes, respectively.

References

1. Israelachvili JN (2011) Intermolecular and surface forces, 3rd edn. Academic, Burlington, MA
2. Leckband D, Israelachvili J (2001) Q Rev Biophys 34(2):105–267
3. Derjaguin B, Landau L (1945) Zhurnal Eksperimentalnoi I Teoreticheskoi Fiziki 15(11): 663–682
4. Verwey EJW, Overbeek JTG, Nes KV (1948) Theory of the stability of lyophobic colloids; the interaction of sol particles having an electric double layer. Elsevier Pub. Co., New York
5. Anderson TH et al (2010) Langmuir 26(18):14458–14465
6. Anderson TH et al (2009) Langmuir 25(12):6997–7005
7. Yu J et al (2011) Nat Chem Biol 7(9):588–590
8. Danner EW et al (2012) Biochemistry 51(33):6511–6518
9. Lum K, Chandler D, Weeks JD (1999) J Phys Chem B 103(22):4570–4577
10. Patel AJ et al (2011) Proc Natl Acad Sci U S A 108(43):17678–17683
11. Bolhuis PG, Chandler D (2000) J Chem Phys 113(18):8154–8160
12. Jamadagni SN, Godawat R, Garde S (2011) Annu Rev Chem Biomol Eng 2(2):147–171
13. Ghosh K, Dill KA (2009) J Am Chem Soc 131(6):2306–2312
14. Israelachvili JN (1973) J Colloid Interface Sci 44(2):259–272
15. Israelachvili JN, Adams GE (1978) J Chem Soc Faraday Trans I 74:975
16. Israelachvili JN (1986) J Colloid Interface Sci 110(1):263–271
17. Chiruvolu S et al (1994) Science 264(5166):1753–1756
18. Kuhl TL et al (1994) Biophys J 66(5):1479–1488
19. Leckband DE et al (1994) Biochemistry 33(15):4611–4624
20. Israelachvili J et al (2010) Rep Prog Phys 73(3):036601

Chapter 3
Effects of Interfacial Redox in Mussel Adhesive Protein Films on Mica

3.1 Introduction

The 3,4-dihydroxyphenylalanine(Dopa)-containing proteins of mussels and sandcastle worms provide attractive design paradigms for engineering synthetic polymers as wet adhesives and coatings [1]. Despite this, a generally accepted explanation of how Dopa interacts with most surfaces is not available. Indeed, given the facile oxidation of Dopa, even the question as to whether Dopa (Fig. 3.1a) is the only interacting functionality on all surfaces remains uncertain. The effect of uncontrollable Dopa redox on the dependability of catechol as an anchoring functionality for polymers is a recognized problem and best illustrated in coatings engineered for superparamagnetic nanoparticles used in magnetic resonance imaging [2]. A one-electron oxidation of Dopa produces a semiquinone (Fig. 3.1a) whereas a two-electron oxidation results in Dopa o-quinone or Dopaquinone (Fig. 3.1b); both have wide-ranging reaction chemistries. Semiquinones are present in the mussel adhesive but their contribution to adhesion is unknown [3]. Dopaquinone is far inferior to Dopa at mediating adhesion to titania and mica surfaces [4, 5], but on amine-functionalized surfaces, it provides up to 200-fold more strength than Dopa itself [4]. In addition, under some solution conditions, tautomers of Dopaquinone, namely Dopaquinone methide (Fig. 3.1c) and α,β-dehydrodopa (Δ-Dopa) (Fig. 3.1d), are more stable than the o-quinone parent. Quinone tautomers were previously detected in oxidized Dopa peptides and proteins [6] and could be associated with structural changes in oxidized adhesive mussel foot proteins such as Mfp-3.

A better understanding of interfacial Dopa chemistry is a crucial prerequisite to engineering the functionality for effective polymer adhesion. In the present study, I deposited thin films of Mfp-3 on mica and tested whether the adhesion and film thickness (hard wall) detected by the surface forces apparatus (SFA) is influenced by the presence or absence of Dopaquinone tautomers in the protein. Dopaquinones were formed in Mfp-3 by autoxidation (raising the pH) or by periodate-mediated oxidation. Protein Dopaquinone tautomerization is intriguing because of its effect on the α-carbons in the peptide backbone and the suggestion that the backbone

J. Yu, *Adhesive Interactions of Mussel Foot Proteins*, Springer Theses,
DOI 10.1007/978-3-319-06031-6_3,

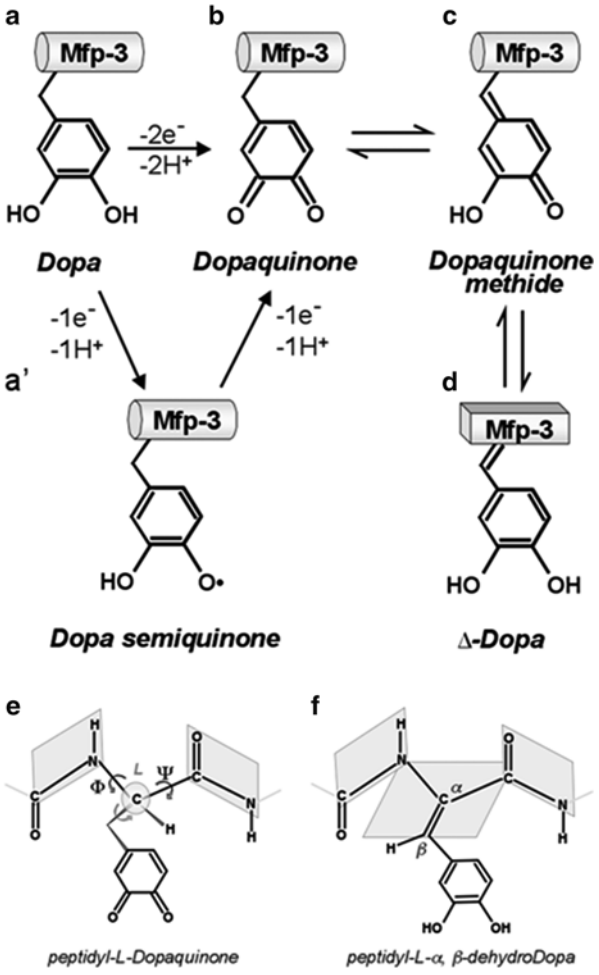

Fig. 3.1 Reaction products for the stepwise 1- and 2-electron oxidation of Dopa (**a**) to Dopa semiquinone (**a'**), Dopaquinone (**b**), and the quinone tautomers, Dopa quinone methide (**c**) and α,β-dehydrodopa (**d**). Dihedral torsional angles are shown around a Dopaquinone side chain (**e**); the essentially planar peptide bonds flank the side chain on both sides. Migration of the double bond to between the α–β carbons in Δ-Dopa abolishes optical activity and places NH, C=O, αC, and βC into the same plane (**f**)

flexibility of adhesive proteins may be adjusted by the selection of different resonance forms of Dopa following oxidation. This runs against the conventional wisdom that oxidation of Dopa-containing proteins serves exclusively as a cross-linking strategy [7, 8].

3.2 The Adhesion Properties of Mfp-3 *Fast* on Mica

A strong adhesion force ~12 mN/m equivalent to an adhesion energy of −2 mJ/m^2 was measured at pH 3 during separation of two Mfp-3 films after a 1 min compression (Fig. 3.2a). Strong adhesion is also consistent with the abrupt jumping apart of two surfaces as manifested by the rapid movement of the fringes of equal chromatic order (FECO). Following introduction of pH 5.5 buffer into the gap solution, the

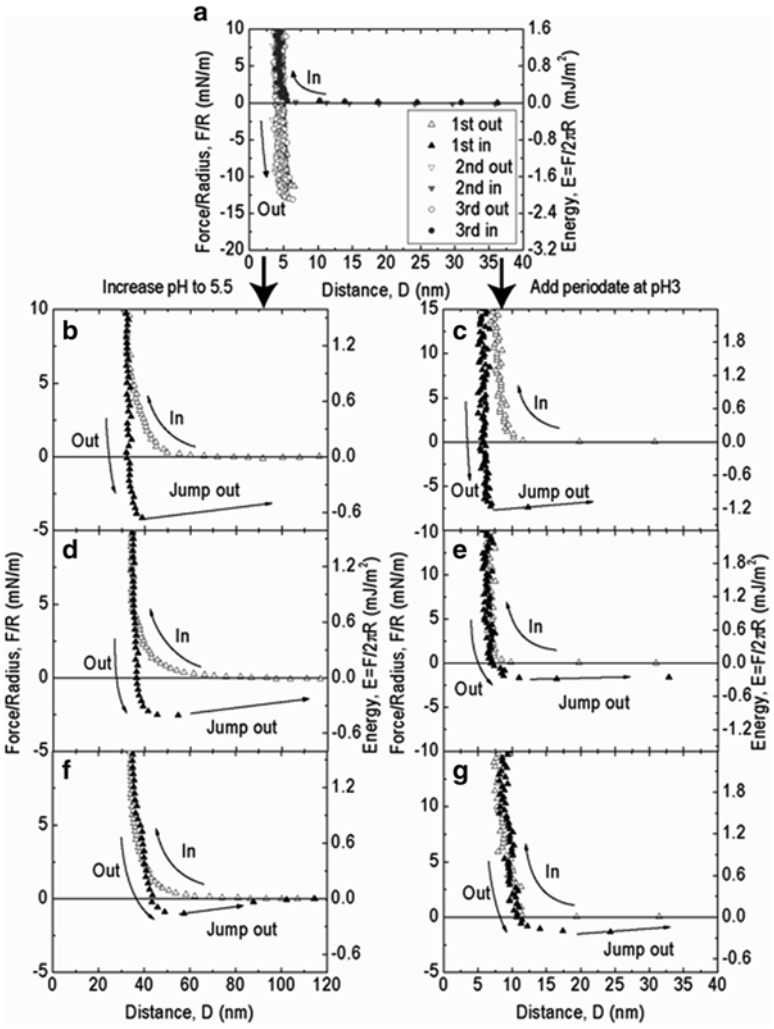

Fig. 3.2 Mfp-3 adhesion and Dopa oxidation. (**a**) The adhesion force of Mfp-3 at pH 3 with three successive approach and separation cycles. (**b**) At pH 5.5, in the first run, an adhesion force of 4.5 mN/m was measured. (**c**) The adhesion decreased to about 2.5 mN/m during the second run and to about 1 mN/m during the third run (**d**). Oxidizing Dopa in Mfp-3 with increasing periodate gives rise to a similar behavior (**e**), (**f**), and (**g**)

surfaces were then brought into brief contact again without changing the contact position. An adhesion force of 4.5 mN/m was measured at pH 5.5 (Fig. 3.2b), decreasing more than 60 % from the Mfp-3 mica adhesion at pH 3. During a second approach at pH 5.5 followed by separation, the measured adhesion force dropped to only 2.5 mN/m (Fig. 3.2c), and the adhesion associated with a third approach-separation cycle measured only ~1 mN/m (Fig. 3.2d). After this, adhesion exhibited no further change. The pH-dependent decrease in adhesion suggests a pH-dependent chemical

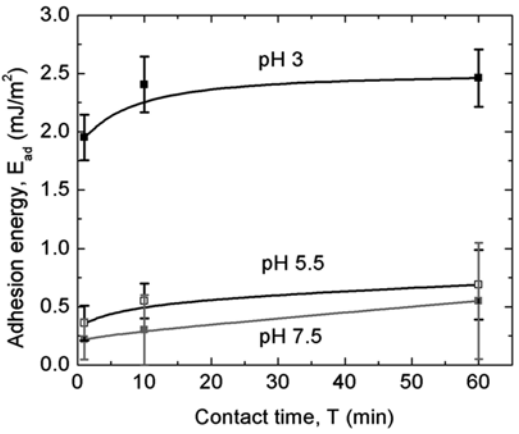

Fig. 3.3 The adhesion energy of the Mfp-3 film and mica as a function of contact time at pH 3, 5.5, and 7.5. At all pHs tested, the adhesion energy slightly increases with contact time. Error bars are the standard deviation of 9–12 measurements for 1 min test and 4–6 measurements for 10 and 60 min test

or structural change in Mfp-3. The most likely chemistry involved is Dopa oxidation. Dopa is known to be unstable at elevated pH, undergoing facile oxidation to Dopaquinone [4, 5, 9]. As Dopaquinones accumulate in Mfp-3, adhesion is diminished with each successive approach and separation cycle and/or time lapsed.

The adhesive strength of Mfp-3 to mica was found to increase with the time of the film in contact with both mica surfaces (Fig. 3.3). When the two surfaces were left in contact for 10 min, the adhesion energy increased to $W_{ad} = -2.4$ mJ/m^2. However, there is no obvious difference in adhesion energy between 10 and 60 min contact time, indicating that the adhesion energy rapidly reaches a plateau. The increase of adhesion energy with contact time is likely due to the rearrangement of the Dopa residues in Mfp-3 chains under confinement. At short contact time, the Dopa residues are likely to be orientated in all the directions, and some of them are not able to bind to the other mica surface due to the steric confinement of the protein chains. Given enough contact time, the protein chains can rearrange their configuration, so more Dopa residues can adhere to the other mica surface. Another plausible explanation is since the protein film was deposited before the SFA experiment, most Dopa residues might adhere to one mica surface during short time contact. A longer contact time gives the Dopa residues a better chance to bind to the other mica surface. Therefore the system is closer to the equilibrium state. Both explanations could lead to a higher adhesive strength with a longer contact time. Once the system reaches its equilibrium state, increasing the contact time does not help increase the strength of adhesion; therefore the adhesion reaches its plateau. In both pH 5.5 and 7.5, the adhesive strength is found to slightly increase with the contact time, but still an order of magnitude lower than the strength measured at pH 3.

3.3 The Effect of Dopa Oxidation

To explore the hypothesis that Dopa oxidation is coupled with a loss in adhesion to mica, a controlled Dopa oxidation experiment was done by adding periodate at pH 3 where Dopa undergoes negligible autoxidation (Fig. 3.2e, f). Periodate, a strong

2-electron oxidant, stoichiometrically oxidizes catechols including Dopa to o-quinones [6, 8]. After achieving a Dopa-mica adhesion at pH 3 of more than 12 mN/m, 200 pmol of periodate (20 μL) was injected into the gap between the Mfp-3 films. Adhesion dropped to 7.5 mN/m in the first approach-separation cycle following injection and further to 1.5 mN/m during the second force cycle. No further decrease in adhesion was observed during subsequent approach-separation cycles. The periodate results support the notion that oxidation of Dopa to Dopaquinone decreases Mfp-3 adhesion to mica at pH 5.5 and 7. The obvious parallels between increasing the pH from 3 to 5.5 of the gap solution and periodate addition at pH 3 suggest that significant Dopa oxidation happens even at pH 5.5 in the SFA. In solution at pH 5.5, Dopa is ordinarily stable for hours, not minutes. In contrast, at seawater pH ~8 and saturating levels of dissolved oxygen, the oxidation of Dopa to quinone is nearly spontaneous [10].

3.4 Dopaquinone Tautomerization

The SFA data reveal a second important trend: the hard wall, an indicator of repulsive interactions and an approximation of the hydrodynamic diameter of Mfp-3, changed dramatically with pH. The film thickness of Mfp-3 on mica at pH 3 was just ~3 nm (Fig. 3.4a). After increasing the pH of the gap solution to 7.5 followed by a short equilibration time, repulsion was first noticeable at a distance of 40 nm during the approach, with an increase in the hard wall to ~20 nm (Fig. 3.4a). The hard wall increase suggests that the Mfp-3 film expands at higher pH. I know of only two chemical pathways relevant to quinone formation in Mfps in this pH range: (1) cross-linking and (2) the tautomerization of the Dopaquinone to Δ-Dopa. Cross-linking is not a plausible scenario for swelling since dilute Mfp-1 in solution undergoes a significant diminution in hydrodynamic radius upon oxidation [11] and cross-linked Mfp-1 films exhibit an irreversible decrease in film thickness as measured by surface plasmon resonance and the quartz crystal microbalance [12]. In contrast, the hard wall increase measured here was largely reversible and thus is more consistent with tautomerization than cross-linking. The tautomerization involves migration of the double bond from the quinone nucleus via the quinone methide to the alpha carbon in the backbone (Fig. 3.1c, d). At pH 7, the Δ-Dopa tautomer is favored, whereas at pH 3 the Dopaquinone prevails [6]. The reversible reduction in the hard wall from 20 to 10 nm by decreasing the pH of the gap solution from 7.5 to 3 is consistent with the reversibility of quinone tautomers but does not prove their involvement (Fig. 3.4a).

Tautomerization of Dopaquinone to Δ-Dopa needs a Lewis base to extract the acidic proton on the αC (Fig. 3.1e, f) [6]. In our experiments, acetate and phosphate buffers, certain Mfp-3 side chains, and even the mica surface [13] itself could act as Lewis bases to catalyze the rearrangement. UV–Vis spectra were performed to test whether the Dopaquinone to Δ-Dopa tautomerization occurs in bulk Mfp-3 solution upon Dopa oxidation. Due to the precipitation of Mfp-3 at near-neutral pH, UV–Vis readings were only reliable up to pH 5.5. Dopa oxidation was enhanced at pH 5.5

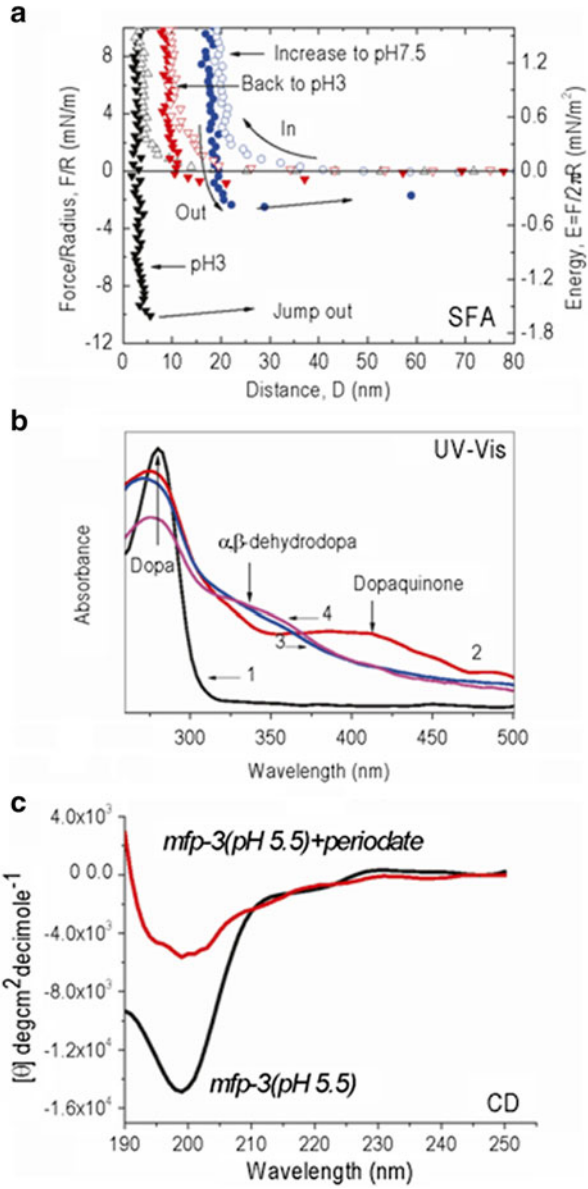

Fig. 3.4 The change of the structure of Mfp-3 with different pHs. (**a**) After increasing the pH of the gap solution from 3 to 7.5, the film thickness measured by the SFA increased from 3 nm to about 20 nm. The hard wall of the protein layer was shifted back to 10 nm when the pH of the gap solution was brought back to 3, but no strong adhesion recovery occurred. (**b**) UV–Vis spectral sequences obtained during the oxidation of 1 mg/mL Mfp-3 by excess periodate in acetate buffer at pH 5.5. Curve 1 (*black*): without periodate; curve 2 (*red*): after adding periodate within the mixing time; curve 3 (*blue*): 30 min; curve 4 (*purple*): 100 min. The peaks around 320 ~ 330 nm and 390 ~ 400 nm increase and decrease, respectively, in absorbance with time. (**c**) CD spectrum of 0.3 mg/mL Mfp-3 in PBS buffer at pH 5.5 (**a**) before and (**b**) after adding excess periodate

(acetate buffer) by adding excess periodate. After periodate addition, a typical quinone spectrum ($\lambda_{max} \approx 390 \sim 400$ nm) developed within the mixing time (Fig. 3.4b). As the oxidation proceeded, the quinone peak decayed, and an increase in absorbance at about 320 ~ 330 nm occurred; this is the characteristic maximum for Δ-Dopa and is consistent with Dopaquinone tautomerization to Δ-Dopa in a low molecular weight peptide [6]. However, in contrast to the SFA experiments,

periodate addition to the bulk solution reaction system was necessary to observe detectable oxidation. The greater susceptibility of Mfp-3 to oxidation in the SFA compared with bulk solution is intriguing and worthy of greater scrutiny. Perhaps the confinement of Mfp-3 between mica surfaces during an SFA experiment enhances its oxidation kinetics [14]. An even more promising possibility could be mechanochemistry, i.e., that a mechanical deformation of Mfp-3 enhances Dopa oxidation. For example, during wood milling, lignins are degraded to benzoquinones [15], and free radicals are generated from catechols during stirring [16].

Considering the double bond between αC and βC atoms, the conformational flexibility of the protein backbone as well as the Δ-Dopa side chain is likely to be more restricted. Without periodate addition, circular dichroism of Mfp-3 exhibits an ellipticity suggestive of random coil structure. After adding periodate to Mfp-3, the ellipticity at 199 nm decreased more than 60 %, indicating a loss of protein conformational flexibility and reduced optical activity (Fig. 3.4c).

In the absence of folding, reduced flexibility of the protein backbone should increase the hydrodynamic size of the protein molecule. The increase in the hydrodynamic dimensions of Mfp-3 was confirmed by dynamic light scattering (DLS). From DLS analysis, Mfp-3 has a hydrodynamic radius of about 1–2 nm or a diameter of ~2–4 nm at pH 3. This diameter approximates the film thickness of the Mfp-3 layer (~3–4 nm) measured by SFA experiment at the same pH (Fig. 3.4a). At pH 5.5, however, the hydrodynamic radius remains at 1–2 nm, much less than the value deduced from SFA measurements (thickness 30–40 nm), and as already mentioned, is attributed to confinement effects in the SFA. Upon raising the pH to 7.5 or adding periodate to pH 5.5 buffer, the hydrodynamic radius of Mfp-3 increased abruptly to 10–25 nm. Dialysis of a solution of Mfp-3 at pH 7 against acetic acid buffer at pH 3 decreased the hydrodynamic radius of Mfp-3 to 4–6 nm. Thus, the DLS-determined increase in hydrodynamic radius following Dopa oxidation also quantitatively agrees with observations from SFA experiments. Although oxidation of Mfp-3 in bulk solution is not necessarily a good approximation of Mfp-3 reactivity on mica surfaces during SFA experiments, it still provides a reasonable basis for assessing the role of Dopa oxidation and quinone tautomers in relation to the adhesion loss and hard wall increase with pH.

3.5 The Binding Mechanism of Dopa to the Mica Substrate

Freshly cleaved mica surfaces are known to consist of chemically inert polysiloxanes, and there is no evidence for a specific coordination complex as that proposed between Dopa and titania surfaces [17]. The moderate adhesion of Mfp-3 to mica is probably due to hydrogen bonding between the bidentate OH groups of the catechol and the O atoms in the mica crystal. The fit should be a snug one as the distance between adjacent O atoms in the mica crystal (~0.28 nm) is about the same as the distance between OH groups in Dopa, ~0.29 nm [5]. As predicted by Bell theory and by analogy to the A-T pairs in DNA, the well-oriented bidentate hydrogen

bonding ($E = \sim -28kT$) of Dopa to mica should have a binding lifetime ($\tau = \tau_0 e^{-E/kT}$) that is 10^6 times as long as the monodentate form ($E = \sim -14kT$) [18].

At pH 3, maximal adhesion energy measured between an Mfp-3-coated mica surface and bare mica after a 60 min contact time is $E_{ad} = -2.5$ mJ/m^2. Typically, the surface area of a mica sheet glued to the SFA cylindrical support is about 1 cm^2. Assuming every molecule in the 20 μL of Mfp-3 solution (20 μg/mL) is adsorbed to mica would deposit about 5.7×10^{-11} mol Mfp-3s on each surface with a corresponding Dopa density of about 5.7×10^{-6} mol/m^2. Although we do not know the actual adsorption efficiency of Dopa to each mica surface, a 50 % adsorption to each surface, the maximum possible amount of Dopa in direct adhesive contact with the mica surface, would give a lower boundary for the Dopa-mica binding of 0.87 kJ/mol. This number is an order of magnitude smaller than the hydrogen bond energy, typically 10–40 kJ/mol. Assuming a lower coverage of 10 %, for example, would give a higher binding, i.e., 4.4 kJ/mol, and may be more realistic.

3.6 The Importance of Dopa Interfacial Redox

Dopa redox plays a dual role in wet adhesion and cohesion within mussel plaques. Our SFA results indicate that Dopa oxidizes to Dopaquinone at even moderately acidic pH, causing a significant drop in adhesion. Once Dopaquinone forms, it quickly undergoes tautomerization to Δ-Dopa, which abolishes side-chain rotation and optical activity in the alpha carbon (Fig. 3.1f). The reaction has also been observed in some Dopa-PEG constructs [19]. Because Dopaquinone tautomerization to Δ-Dopa in Dopa-containing proteins and peptides imposes severe local configurational constraints, it would be expected to increase the hydrodynamic radius of a single protein chain. The double bond between the α and β carbons (Fig. 3.1f) puts them in the same plane as the α-amine and carbonyl groups of the backbone with 120° angles around the sp^2 α-carbon and a loss of optical activity [20]. Given the ten fairly evenly distributed Dopa residues in the Mfp-3 sequence [21], converting all of these to Δ-Dopa would be expected to decrease entropy in the chain and perhaps impose a new secondary conformation. The nature of this conformation in Mfp-3 is not known at this time but reasonable conjecture is possible. Mathur et al. [21] prepared a synthetic octapeptide with alternating Δ-Phe residues that exhibited a distinct preference for a 3_{10} helix. This resembles an α-helix in being internally H-bonded but with fewer amino acids (i to $i+3$) between each donor-acceptor pair [22].

It is not currently known whether Δ-Dopa formation in Mfp-3 on surfaces is adaptive or adventitious. The former would require a certain degree of local redox and pH control. Mussels can retard oxidative losses in the plaque by co-secreting a thiol-containing protein antioxidant with Mfp-3 and Mfp-5 at relatively low pH regimes during plaque deposition [23]. A spatially tuned control of Δ-Dopa formation would enable an extraordinary versatility in how the proteins are packed as they approach a solid surface. Indeed, the obvious porosity gradient in the plaque could be taken as evidence of such versatility [24].

3.7 Experimental Section

Materials: Mfp-3 was purified according to a procedure previously described [21]. Purified Mfp-3 performs consistently by SFA after storage for 100 days at pH 3 and −50 °C. Before the experiment, 20 μL of Mfp-3 solution (20 μg/mL) was injected onto one or both mica surfaces. After allowing 30 min absorption followed by rinsing with buffer, the two surfaces were then transferred into an SFA chamber with a droplet of buffer in between the surfaces for measurement. The volume of the droplet solution is about 50 μL. Buffer preparation: 0.1 M acetic acid (EMD Chemicals, Gibbstown, NJ) and 0.25 M potassium nitrate (Aldrich, St. Louis, MO) (pH 3); 0.1 M sodium acetate (EM Science, Gibbstown, NJ) and 0.25 M potassium nitrate titrated by acetic acid (PH 5.5); 0.016 M potassium phosphate monobasic (Mallinckrodt, Hazelwood, MO) and 0.084 M potassium phosphate dibasic (EMD Chemicals, Gibbstown, NJ) (PH 7.5). Milli-Q water (Millipore, Bedford, MA) was used for all the glassware cleaning and solution preparation.

UV–Vis Spectrophotometry: UV–Vis spectra were obtained using a Nanodrop 1000 spectrophotometer (Thermo Fisher Scientific, Wilmington, DE). 20 μL of 1 mg/mL Mfp-3, caffeic acid, and hydrocaffeic acid were made in acetate buffer at pH 5.5, respectively (0.1 M sodium acetate titrated by acetic acid). Excess sodium periodate was used to oxidize hydrocaffeic acid and Dopa in Mfp-3.

Circular Dichroism Spectroscopy: Circular dichroism (CD) measurements were performed on an OLIS RSM circular dichroism spectropolarimeter. The cell was maintained at 25 °C using a quantum temperature controller. Far-UV (250–190 nm) scans were performed in a micro cell (with a path length of 0.05 cm) that required only 300 μL of solution. The computer-averaged trace of ten scans was employed in all calculations. Signal due to solvent was subtracted. 0.3 mg/mL of Mfp-3 was measured in PBS buffer at pH 5.5 before and after adding 10 μL of 3.2 mg/mL $NaIO_4$. The data were normally plotted as mean-residue-weight ellipticity ([θ]; units.degrees.cm^2 dmol^{-1}) versus wavelength in nm, calculated via the following equation:

$$\theta = \frac{\theta_{\text{obs}} m.r.w.}{10cD}, \tag{3.1}$$

where θ_{obs}. is the observed ellipticity in degrees, *m.r.w*. is the mean residue weight, *c* is the concentration in g/mL, and *D* is the path length in cm.

DLS: DLS was used to evaluate the hydrodynamic dimensions of the protein samples. The hydrodynamic radius of Mfp-3 at pH 3 (acetic acid), 5.5 (sodium acetate), 7.5 (phosphate), and pH 5.5 (phosphate) was determined after adding excess amount of oxidant $NaIO_4$ at 20 °C using a Dynapro DLS temperature-controlled microsampler with an 824.7 nm laser diode (Protein Solutions, Charlottesville, VA). DLS scattering counts were recorded every 10 s (10 acquisitions/sample) and scattering intensity data were processed using Dynamics Dynapro Control software v.6.3.40.

References

1. Dalsin JL et al (2003) J Am Chem Soc 125(14):4253–4258
2. Amstad E et al (2009) Nano Lett 9(12):4042–4048
3. Sever MJ et al (2004) Angew Chem Int Ed 43(4):448–450
4. Lee H, Scherer NF, Messersmith PB (2006) Proc Natl Acad Sci U S A 103(35):12999–13003
5. Anderson TH et al (2010) Adv Funct Mater 20(23):4196–4205
6. Rzepecki LM, Nagafuchi T, Waite JH (1991) Arch Biochem Biophys 285(1):17–26
7. Waite JH (1990) Comp Biochem Physiol B Biochem Mol Biol 97(1):19–29
8. Liu B, Burdine L, Kodadek T (2006) J Am Chem Soc 128(47):15228–15235
9. Yu ME, Deming TJ (1998) Macromolecules 31(15):4739–4745
10. Proudfoot GM, Ritchie IM (1983) Aust J Chem 36(5):885–894
11. Haemers S et al (2002) Langmuir 18(12):4903–4907
12. Hook F et al (2001) Anal Chem 73(24):5796–5804
13. Giese RF, Wu W, van Oss CJ (1998) J Disper Sci Technol 19(6–7):775–783
14. Santiso EE et al (2007) Appl Surf Sci 253(13):5570–5579
15. Wu ZH, Sumimoto M, Tanaka H (1995) J Wood Chem Tech 15(1):27–42
16. Tipikin DS, Lebedev YS, Rieker A (1997) Chem Phys Lett 272(5–6):399–404
17. Li SC et al (2010) Science 328(5980):882–884
18. Israelachvili JN (2011) Intermolecular and surface forces, 3rd edn. Academic, Burlington, MA
19. Lee BP, Dalsin JL, Messersmith PB (2002) Biomacromolecules 3(5):1038–1047
20. Pieroni O et al (1993) Biopolymers 33(1):1–10
21. Zhao H, Waite JH (2006) J Biol Chem 281(36):26150–26158
22. Mathur P, Ramakumar S, Chauhan VS (2004) Biopolymers 76(2):150–161
23. Zhao H et al (2006) J Biol Chem 281(16):11090–11096
24. Tamarin A, Lewis P, Askey J (1976) J Morphol 149(2):199–221

Chapter 4
Antioxidant is a Key Factor in Mussel Protein Adhesion

4.1 Introduction

Moisture is the nemesis of strong polymer adhesion to polar surfaces. Despite this, marine mussels achieve durable underwater adhesion using a suite of proteins that are peculiar in having high levels of Dopa [1, 2]. The recent demonstration that a single tethered Dopa residue adsorbed to titania in water requires a breaking force of nearly 1 nN and is completely reversible [3] has spawned the design of many synthetic polymers with Dopa-like side chains for diverse applications [4–7]. Despite its many virtues as a sticky side chain [8], Dopa has a troubling side that presents significant challenges to its use, i.e., coupled to the reduction of atmospheric oxygen, it is readily oxidized to Dopaquinone. Dopaquinone formation diminishes adhesion on TiO_2 by at least 80 % and is very prone to further chemical modification including protein cross-linking reactions [3]. Given the little effort devoted so far to controlling the stability of Dopa, it is not surprising that the range of adhesive strengths reported for Dopa-containing polymers varies widely [9–12]. At the single-molecule level, for example, the reported breaking force of Dopa adsorbed to titania at pH 7.5 differed by an order of magnitude in two reports [3, 13].

The holdfast or byssus of a California mussel (*Mytilus californianus* Conrad) resembles a bundle of threads, each of which is distally tipped with a flared adhesive plaque (Fig. 4.1a). About ten plaque proteins have been characterized and half of these are unique to the plaque whereas the others are distributed in both threads and plaques [14]. The mussel assembles each new plaque in a few minutes from proteins stockpiled in its foot. The first proteins the foot squirts onto the surface of a rock are mussel foot proteins Mfp-3 and Mfp-5 with Dopa contents of 20 mol% and 30 mol%, respectively [1, 2] (Fig. 4.1b, c). With the surrounding seawater at pH ~8 and saturating levels of dissolved oxygen, the 2-electron oxidation of Dopa to Dopaquinone is predicted to be highly favorable (Fig. 4.1d) but is retarded to a significant extent in the native adhesive footprints of mussels [1, 2]. Here I investigated whether reduced Dopa is necessary for good adhesion to a mineral such as mica and, if so, how the redox of these oxidation-prone proteins is manipulated.

J. Yu, *Adhesive Interactions of Mussel Foot Proteins*, Springer Theses,
DOI 10.1007/978-3-319-06031-6_4,

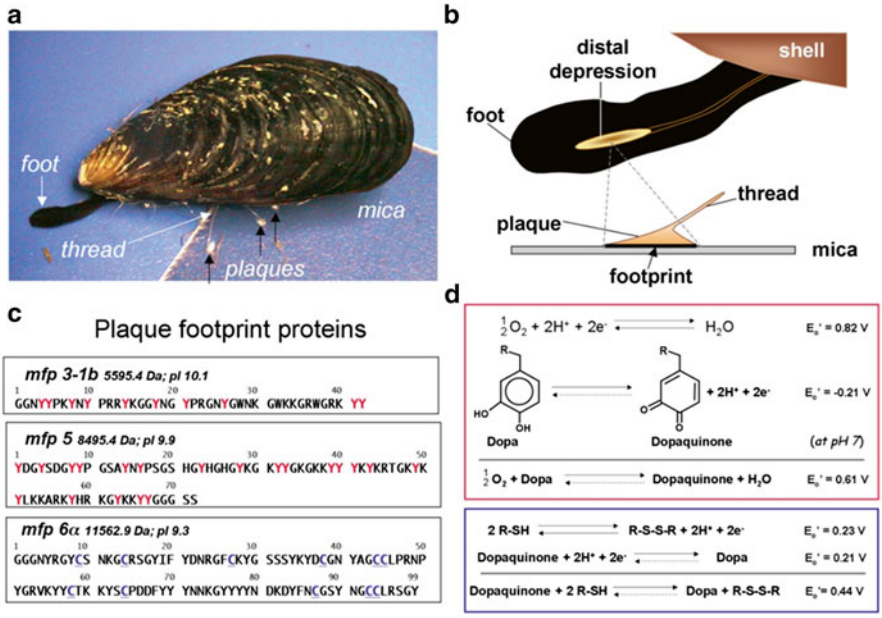

Fig. 4.1 Byssal adhesion in the California mussel *Mytilus californianus*. (**a**) An adult mussel attached to a mica sheet by a byssus containing three threads. Extended foot is making a new plaque and thread; (**b**) zoom of a foot viewed from the underside showing the distal depression lifting off from a completed plaque. The footprint denotes the distalmost part of each plaque in intimate contact with the surface; (**c**) primary sequence of selected footprint protein variants of Mfp-3 (*>25 known variants*), Mfp-5 (*2 known variants*), and Mfp-6 (*5 known variants*); the high proportion of Dopa (*red* Y) and cysteine (*blue* C) in mefp-3, Mfp-5, and Mfp-6, respectively, is as shown. Masses were calculated from the cDNA-deduced sequences. (**d**) Standard oxidation-reduction half-reactions of oxygen, Dopa, and cysteine thiols at pH 7 (*from ref 19*). *Dashed arrows* denote only partially reversible reactions

4.2 The pH of Mussel Adhesive Protein Secretion

The adhesion of *M. californianus* was investigated in two parts: first, solution conditions in the foot during plaque formation were determined, and second, using the surface forces apparatus (SFA), I measured the adhesive interactions between purified Mfps and mica at three pHs [15]. With respect to solution conditions, researchers have always assumed that sessile marine organisms attach to surfaces at seawater pH (≈ 8.2). Each adhesive plaque is injection molded by the mussel into a small dimple known as the distal depression located near the tip of the foot (Fig. 4.1b); the depression is placed like an inverted cup over a selected surface and a minute or so later, proteins are exuded from pores in the depression ceiling. Given the unpredictability of byssal thread formation by captive mussels, we gave up the idea of

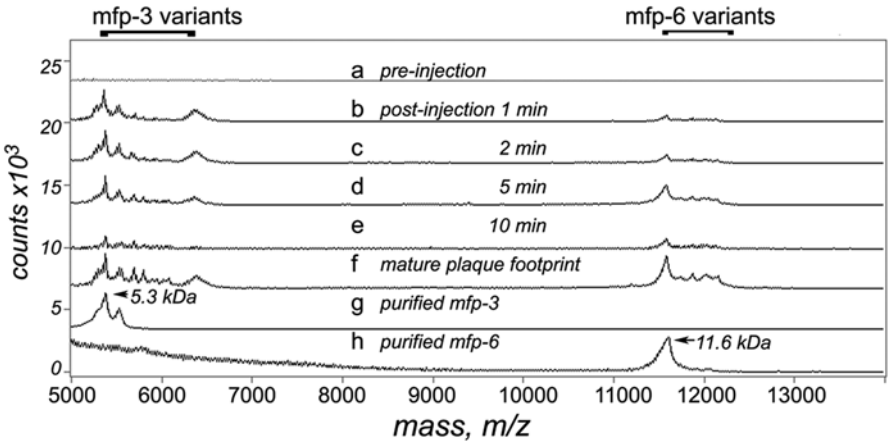

Fig. 4.2 Mass analysis of proteins in the distal depression during plaque formation induced by stimulating the pedal nerve. (**a**) Pre-injection swab of proteins in the distal depression; (**b**) 1 min post-injection swab of distal depression; (**c**) 2 min post-injection swab; (**d**) 5 min post-injection swab; (**e**) 10 min post-injection swab; (**f**) proteins of a mature plaque footprint; (**g**) purified Mfp-3 protein variants (5.3 kDa peak mass) used in SFA experiments; (**h**) purified Mfp-6 variants (11.6 kDa) used in SFA experiments. Note absence of Mfp-5 (9.5 kDa) which requires much higher laser power to desorb during analysis by MALDI

sampling solution conditions in the distal depression during the natural deposition of a plaque. Instead, changes occurring following byssus secretion induced by injecting a potassium chloride solution into the pedal nerve were measured. Previous reports maintain that the products of induced and natural secretion are indistinguishable [16, 17]. To confirm these claims, we sampled the distal depression of a mussel foot for proteins before injection and at 1, 2, 5, and 10 min post-injection by MALDI TOF mass spectrometry (Fig. 4.2a–e). Mfp-3 variants, specifically Mfp-3-1α (5.3 kDa), Mfp-3-1β (5.4 kDa), Mfp-3-2 (5.5 kDa), and Mfp-3-3α (6.6 kDa) [1], are secreted first followed closely by Mfp-6 (~11.6 kDa). The cumulative pattern of induced secretion is nearly identical to the distribution of proteins in a natural plaque footprint (Fig. 4.2f). The estimated final molar ratio of Mfp-3/Mfp-6 averages about 2.5:1, but whether this ratio is fixed or adjustable on different surfaces requires further investigation.

With a calibrated microelectrode inserted into the distal depression (1–2 mm diameter in adult *M. californianus*), we followed the time course of pH after injecting KCl into the pedal nerve, known to induce plaque and thread formation. Just prior to the secretion of plaque proteins, the pH of the distal depression dropped by an average of 1.5 pH units (SD ± 0.3 $n = 15$) from a resting pH of pH 7.3 to 5.8 within 2 min of induction. Given how densely adhesive proteins fouled the microelectrode tip, the pH decrease of 1.5 units should be considered as a minimum. Conductivity tests of the induced byssal secretions of five mussels indicated an average ionic strength of 80 mM (SD ± 23 mM) compared with ionic strengths of 215 and 700 mM for cytoplasmic fluid [18] and seawater, respectively.

4.3 The Wet Adhesion of Mfp-3 *Fast* on Mica

Using pH regimes ranging from pH 3 to 7.5 at a salt concentration (0.25 M KNO_3) intermediate between the adhesive exudate and seawater, the adhesion of Mfp-3 to mica was tested in the SFA [15]. The greatest adhesion energy ($E \sim -2.0$ mJ/m^2, SD ± 0.3, $n = 6$), observed at pH 3 following the brief contact and separation of two Mfp-3 films (Fig. 4.3), is consistent with Dopa residues that are H-bonded to mica surfaces. Apparently, during contact, Mfp-3 chains already bound to a mica surface rearrange to span the gap to bind another surface. A single Mfp-3 film had a thickness (hard wall) of 5 nm when compressed. The strong adhesion between two Mfp-3 films at pH 3 (Fig. 4.3) underwent a surprising 75 % diminution at pH 5.5 to ~ −0.50 mJ/m^2 (SD ± 0.15, $n = 6$) within a few minutes of raising the pH. When the pH of the gap solution was further increased to 7.5, only weak adhesion remained. Given that the autoxidation of catechols increases with increasing pH [19], I tested whether adhesion loss is correlated with Dopa oxidation. Titration with an oxidant at pH 3 supports this premise (Fig. 4.4). In periodate oxidation, for example, each periodate ion produces a stoichiometric 2-electron oxidation per Dopa [20, 22]. At 600 pmol periodate, adhesion is essentially abolished.

Another pH-dependent change in Mfp-3 is the greater repulsion in films of Mfp-3 at pH 5.5 and 7.5 during approach. Using the hard wall as a measure of repulsion, there is an outward shift from 5 to 35 nm at pH 5.5, and 50 nm at pH 7.5 (Fig. 4.3a). The greater repulsion at higher pH could reflect Mfp-3 cross-linking [23] and/or the tautomerization of peptidyl-Dopaquinone to α,β-dehydrodopa, which would have the effect of locking the peptide backbone into a planar double bond at every oxidized Dopa residue [21, 24]. Given its reversibility, tautomerization is the more plausible explanation. Compliant protein chains pulled out normal to the mica surface during separation would be stiffened during the pH-induced oxidation and tautomerization steps, and the stiffened chains would begin resisting compression earlier during the next approach. Antioxidants would reduce quinones and related tautomers back to Dopa and restore chain flexibility.

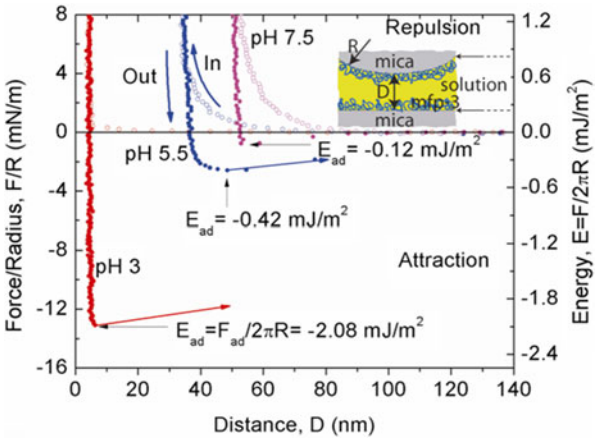

Fig. 4.3 Force-distance profiles of two Mfp-3-coated mica surfaces at different pH. At pH 3 (*red*), up to −13.5 mN/m ($E_{ad} = -2.08$ mJ/m^2) adhesion was measured. The adhesion decreased to about $E_{ad} = -0.42$ mJ/m^2 (*blue*) at pH 5.5. Only a slight adhesion of $E_{ad} = -0.12$ mJ/m^2 was measured when the pH of the gap solution was raised to 7.5 (*magenta*)

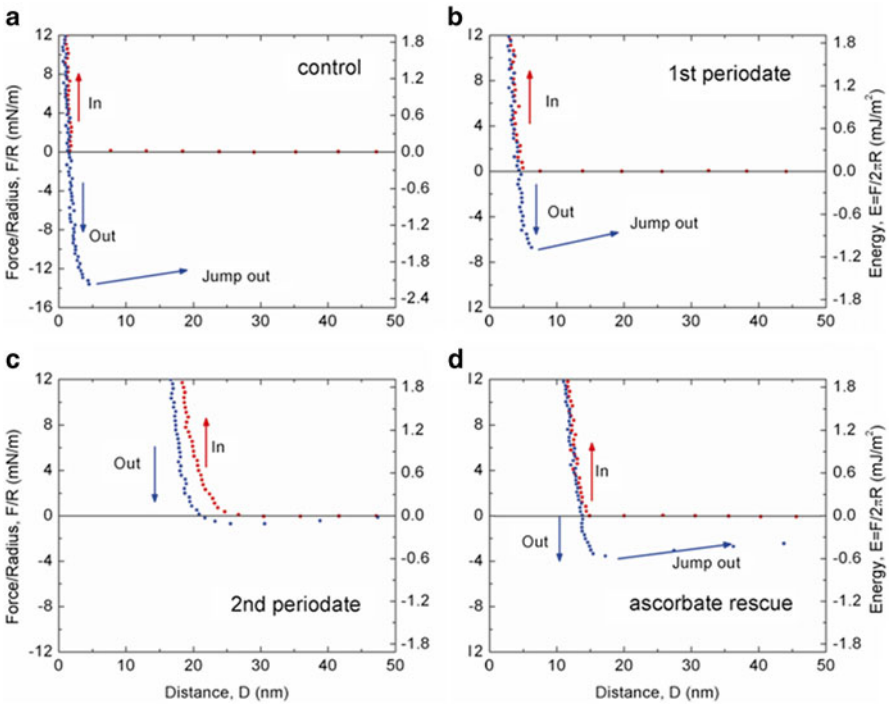

Fig. 4.4 The force-distance profiles of Mfp-3 on mica before and after adding artificial oxidant, $NaIO_4$, and antioxidant, ascorbic acid. (**a**) Mfp-3 on mica at pH 3. (**b**) A 30 % loss of adhesion was measured after adding 400 pmol $NaIO_4$ into the gap at pH 3. (**c**) Near-abolition of adhesion after adding 600 pmol $NaIO_4$ into the gap solution at pH 3. (**d**) Adding 20 μL ascorbic acid (0.25 mM) into the gap solution recovered about 30 % of the adhesion

Clearly, Dopa in purified Mfp-3 is susceptible to oxidation during testing in the SFA. In contrast, however, biochemical analysis of plaques shows that the Dopa content of adhesive proteins such as Mfp-3 and Mfp-5 remains largely intact while they reside in the plaque footprints [1]. Presumably mussels are adding something else to the plaque footprints to stabilize the redox of the adhesive proteins there.

In order to determine whether Dopa oxidization is responsible for adhesion loss and the longer-range repulsion, the effect of oxidants and antioxidants on Mfp-3 adhesion was examined. An artificial oxidant, sodium periodate ($NaIO_4$), was added into the gap of two films of Mfp-3 at pH 3 at which the autoxidation of Dopa is low. Each periodate stoichiometrically oxidizes a Dopa to Dopaquinone. A 45 % loss of adhesion was measured within a few minutes after introducing 400 pmol of periodate into the gap solution between the mica surfaces (Fig. 4.4a, b). An essentially complete adhesion loss as well as a significant increase in repulsion occurred with an additional 200 pmol of periodate (Fig. 4.4c). The correlation between the amount of periodate added into the gap and the decrease of adhesion indicates that the oxidization of Dopa is an important factor in adhesion loss and consistent with the autoxidation at pH 5.5 and 7.5. The shift of the hard wall also supports contribution of chain

stiffening or cross-linking to longer range repulsion. With regard to antioxidants, I introduced ascorbic acid (2.5 nmol) to reduce Dopaquinone in oxidized Mfp-3 and in doing so rescued a substantial proportion of adhesion (Fig. 4.4d).

4.4 Adhesion and the Antioxidant Effect of Mfp-6

In situ matrix-assisted laser desorption mass spectrometry of mussel adhesive footprints and induced adhesive secretion detected Mfp-3 and Mfp-6 variants (Fig. 4.2) [1, 2]. Mfp-6 composition differs from Mfp-3 variants by its low Dopa and high cysteine content [2]. In freshly isolated Mfp-6, of the eleven cysteines known to exist in the protein, two are coupled as a disulfide leaving nine to occur presumably as thiols [1]. These nine thiols are not readily accessible to modification: at best 1–2 thiols can be carboxymethylated with iodoacetamide at pH 7, whereas 4–5 react with Ellman's reagent (Table 4.1). With respect to adhesion in the SFA, Mfp-6 adsorbed to one or both mica surfaces exhibits only weak adhesion (Fig. 4.5).

Given Mfp-6's poor adhesion, I surmised it bestowed other adaptive advantages on mussel attachment. To explore these, two Mfp-3 films were autoxidized at pH 7.5; the gap solution was returned to pH 5.5 by buffer replacement. Adhesion, however, remained unchanged (Fig. 4.6a) suggesting that pH alone is insufficient to reverse the autoxidation of Dopa. About 100 pmol of Mfp-6 was then introduced into the gap at pH 5.5. The films were brought into brief contact and upon separation exhibited an adhesive energy of about -0.70 ± 0.05 mJ/m^2 ($n = 6$), a 130 % recovery of adhesion; following a 60 min contact, there was a 200 % recovery of initial adhesion (Fig. 4.6b). At pH 3, Mfp-6 further increased adhesion of two Mfp-3 films to -1.21 ± 0.05 mJ/m^2 and -1.85 mJ/m^2 after ~1 and 60 min contacts, respectively (Fig. 4.6c). These results resemble, but are more potent than, the effects of ascorbate on adhesion loss (Fig. 4.4d) and implicate Mfp-6 as an antioxidant to restore Dopaquinone to Dopa in Mfp-3.

The mechanism of antioxidant action by Mfp-6 is suggested by its cysteinyl thiol content. I surmised that thiols in Mfp-6 provide reducing equivalents for

Table 4.1 Cysteine detection in purified Mfp-6 (mass 11,887 Da)

Treatments and detection in mol%					
Cys derivative	Untreated Mfp-6	Mfp-6 + Ellman's	Mfp-6 + iodoacetamide pH 7.5	Mfp-6 + DTT iodoacetamide GuHCl pH 7.5	Performate oxidized
Cys-SO_2H	0	0	0	0	10.6 ± 0.4
CM-Cys	0	0	2.5 ± 0.2	4.3 ± 0.2	0
Cystine	1.1 ± 0.2	1.1	1.1 ± 0.2	0	0
NBT	0	4.6 ± 0.2	0	0	0

Comparison of untreated, performic acid-oxidized, and carboxymethylated cysteines in Mfp-6 in mol%. Measurements are means + standard deviation for $N = 4$
DTT dithithreitol, *GuHCl* guanidine hydrochloride

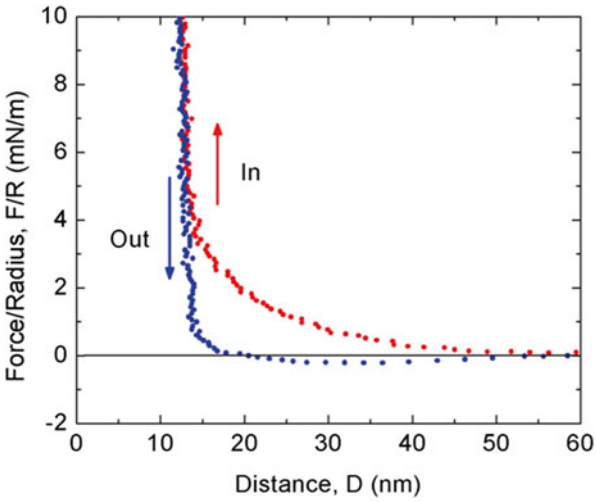

Fig. 4.5 Typical force-distance profile of two Mfp-6-coated mica surfaces. Only weak adhesion was measured during separation following a brief contact. The Mfp-6 deposition was done using the same method demonstrated in the methods section with an Mfp-6 solution of 20 μg/mL

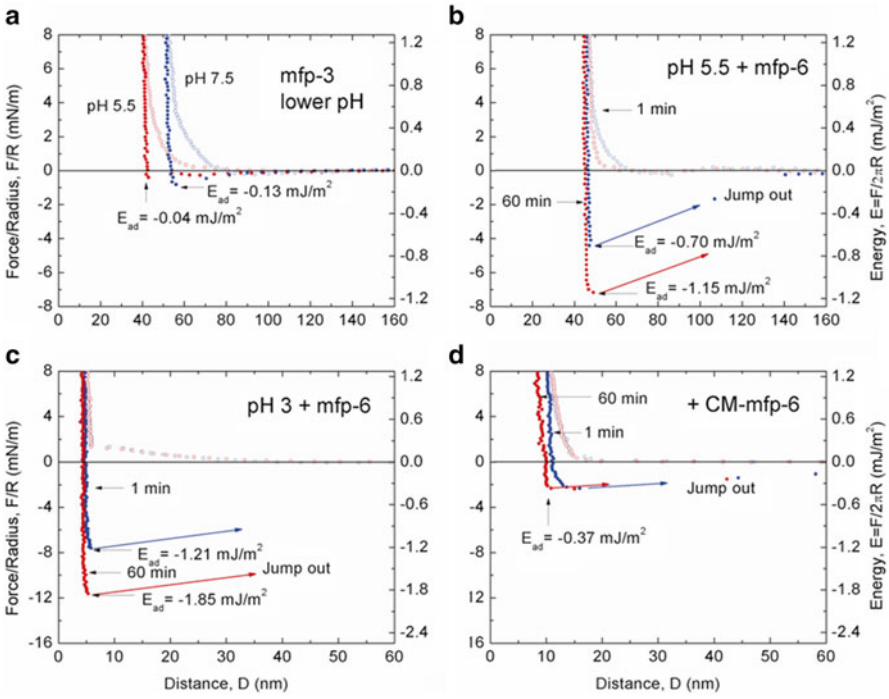

Fig. 4.6 Adhesion of Mfp-3 at different pH values before and after adding Mfp-6. (**a**) Simply decreasing the pH from 7.5 to 5.5 did not recover significant adhesion. (**b**) After injecting Mfp-6 into the gap solution at pH 5.5, an adhesion force corresponding to $E_{ad} \sim -0.7$ mJ/m^2 was measured after keeping the two surfaces in contact for 1 min. The adhesion energy increased to −1.15 mJ/m^2 when the surfaces were in contact for 60 min. (**c**) Even stronger recovery of adhesion was evident after injecting Mfp-6 at pH 3. The adhesion energy was −1.21 mJ/m^2 for 1 min contact and −1.85 mJ/m^2 for 60 min contact. (**d**) Injecting S-carboxymethylated Mfp-6 at pH 3 failed to recover the lost adhesion of Mfp-3

Dopaquinone formed in Mfp-3 (Fig. 4.1d). To test this, accessible cysteinyl thiols in Mfp-6 were S-carboxymethylated with iodoacetate at pH 7.5 (Table 4.1), and the modified protein was then added to films of oxidized Mfp-3 at pH 3. Carboxymethylated Mfp-6's ability to rescue the adhesion of Mfp-3 was at best feeble after a short contact (Fig. 4.6d) and did not improve after a 60 min contact. The slight adhesive rescue suggests that the SH groups were not fully blocked. The failure of carboxymethylated Mfp-6 to rescue the adhesion of Mfp-3 (Fig. 4.6d) supports the premise that cysteinyl residues of Mfp-6 provide a limited pool of reducing thiols to regenerate Dopa from Dopa lost by oxidation to Dopaquinone. As thiolates not thiols are the more strongly reducing, the persistence of reducing activity even to pH 3.0 suggests that the thiols in Mfp-6 have unusually low pK_as.

4.5 Discussion

My results show that a mussel imposes a specific chemical microenvironment on the distal depression of the foot during the initial stages of plaque formation. Niche conditions include an acidic pH and ionic strength only 10–15 % that of seawater. The low pH regime is reminiscent of the proton pumping vacuoles of ascidian vanadocytes, which achieve a pH below 4 [25]. Redox control also appears to be important during adhesion. Use of the SFA to reenact initial molecular events in Mfp-3 adhesion reveals the surprising susceptibility of Dopa residues to oxidation even at pH 5.5. Adhesion loss in Mfp-3 is highly correlated to Dopa oxidation and can be partially counteracted by antioxidants such as ascorbate that reduce Dopaquinone back to Dopa (Fig. 4.6). A fully potent antioxidant effect is produced by adding Mfp-6—a protein that resides naturally in plaques at an abundance about a third that of Mfp-3 and is secreted shortly after Mfp-3. The mechanism of Mfp-6 action is only partially understood. The effect of Mfp-6 carboxymethylation on Mfp-3 adhesion suggests that Mfp-6 action is thiol-mediated involving up to five thiols per molecule [1] (Table 4.1). The thiolate not thiol form is the operative antioxidant group and blocking thiolates diminishes the antioxidant activity of Mfp-6 [25]. Thiolates in Mfp-6 react almost as readily at pH 4–5 as at pH 7.5 suggesting thiol pK_as in Mfp-6 that are substantially lower than typical cysteine pK_as at 8–9. The lowest reported thiol pK_a is 3.5, which occurs at Cys-30 in the sequence CxxC in the redox protein DsbA from *E. coli* [25]. Lowering the thiol pK_a would give Mfp-6 more reducing power for Dopa rescue from Dopaquinone at the pH of plaque formation [25, 26] (Fig. 4.7).

Redox control in Mfp-3 must be considered in the context of plaque formation. A small volume (~10–20 μL) of fluid containing Mfp-3 variants is secreted into the distal depression (Fig. 4.7a) at a $pH \leq 5.5$. The proteins are rapidly adsorbed onto the mica surface by Dopa-mediated H-bonds (Fig. 4.7a). Each Mfp-3 has ten Dopa residues. Given the small size of Mfp-3 (5–6 kDa) and its extended unstructured conformation, adsorption is rapid and irreversible [15, 27]. The nearly identical spacing (0.29 nm) between the ortho hydroxyl groups in Dopa to the O-O distances (0.28 nm)

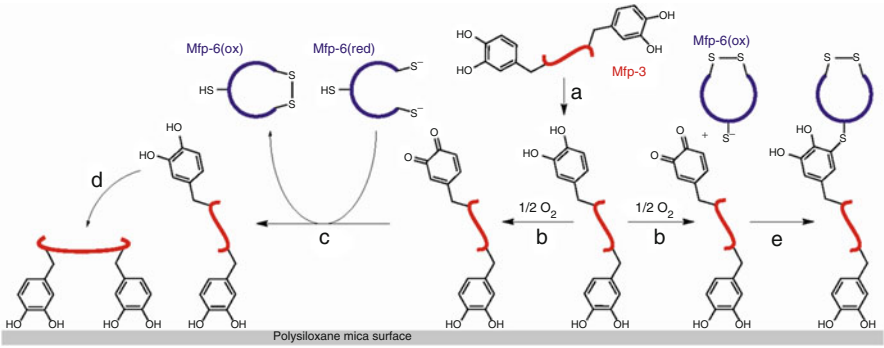

Fig. 4.7 Redox control and the stepwise adsorption and cross-linking of Mfp-3. (**a**–**e**) Mfp-3 variants are secreted into the distal depression (**a**) and partially adsorbed by Dopa-mediated H-bonds to the mica surface. The oxidation of unadsorbed Dopa to dopaquinone (**b**) is counteracted by reducing thiolates (**c**) in Mfp-6, which enables enhanced adsorption (**d**). Depletion of thiolate pairs in Mfp-6 transforms Mfp-6 into a cross-linker with Mfp-3 (**e**). *Red* reduced, *ox* oxidized

of the polysiloxane surface of mica [27] probably shields Dopa H-bonded to mica from oxidation (Fig. 4.6b). As predicted by Bell theory and by analogy to the A-T pairs in DNA, the well-oriented bidentate hydrogen bonding ($E = \sim -28kT$) of Dopa to mica should have a binding lifetime ($\tau = \tau_0 e^{-E/kT}$) that is 10^6 times as long as the monodentate form ($E = \sim -14kT$) [28]. In contrast, the Dopa residues not initially adsorbed are prone to oxidation (Fig. 4.7b). This loss is transiently repaired by the thiols of Mfp-6 (Fig. 4.7c) enabling fuller adsorption of Mfp-3 (Fig. 4.7d). However, keeping all Dopa reduced in the plaque cannot be sustained for long by Mfp-6. As the population of available reducing thiols dwindles, the coupled thiol-quinone redox system accumulates S-cysteinyl Dopa adducts (Fig. 4.7e). As shown in supporting data (Fig. 4.8), the quinone reducing action of thiolates consists of two steps: a nucleophilic attack of the quinone by the first thiolate anion to form S-cysteinyl-Dopa adducts, followed by the attack of the thioether by the second thiolate anion to form a disulfide and Dopa [29]. This scheme is consistent with the detection of 0.5–1.0 mol% 5-S-cysteinyl-Dopa cross-links in acid-hydrolyzed plaques [1].

The emerging picture is that Mfp-6 may be efficiently adapted to be first an antioxidant and then a cross-linking partner for Mfp-3, the latter function being crucial for improving cohesion among the plaque proteins [30]. It must be stressed, however, that cohesive interactions between plaque proteins do not depend solely or predominantly on quinone adducts. The intrinsic protein–protein binding energy between Mfp-5 and Mfp-2 is independent of quinones and requires up to 1.5 mJ/m^2 to break [15]; equally important, the iron-mediated bridges between Dopa residues in Mfp-2 and Mfp-1 range from 2 to 5 mJ/m^2 [2, 31].

Redox regulation of cellular compartments such as the nucleus, cytosol, Golgi, and the periplasmic space using glutathione and thioredoxins is well known [25, 26, 32]. Secreted variants of the same or similar antioxidants are also used to regulate redox of extracellular tissues and plasma [33]. Byssal plaque formation is an unprecedented example of redox control beyond the living organism. Perhaps

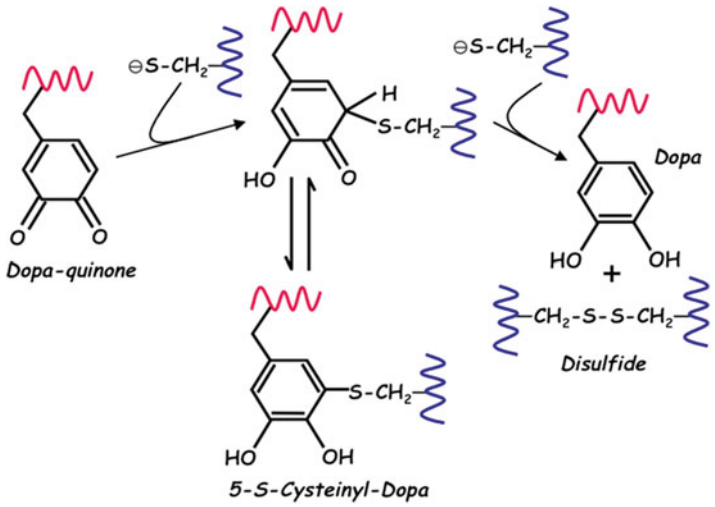

Fig. 4.8 Reaction mechanism of quinone reduction by thiolates. Reaction begins with a nucleophilic attack on the quinone by the first thiolate forming a nonaromatic intermediate adduct. The second thiolate then attacks the thioether adduct thereby eliminating the disulfide and regenerating Dopa

because of the unusual requirements of this adaptation, the cDNA-deduced sequence of Mfp-6 has no homology with any proteins in the database (BLAST). Although Mfp-6 is 11 mol% cysteine, only 1–3 cysteines are thiols, two form a disulfide, and the remaining seven occur in an unknown nonreducible form. The low thiol level defining the reducing power of Mfp-6 in *Mytilus* is not representative of all mussels; the cysteine thiol content of plaque proteins from other mussel species (e.g., *Perna*) can be as high as 20 mol% [32]. There is no evidence so far that the thiols of Mfp-6 can be regenerated from disulfides as they are within compartments of living cells.

With regard to promoting energetic surface interactions, I have treated reduced Dopa as the only productive interaction on mica. However, Dopaquinone formation is also known to be an asset for adhesion particularly on protein- and amine-functionalized surfaces [3, 7]. In this case, covalent Michael-type additions and aryl coupling reactions are proposed to occur across the interface. A provocative question for future research to consider is whether mussels can tune the interfacial redox environment to favor quinones on organic surfaces and Dopa on minerals and metals. Mussels certainly adhere well to both, and understanding the details of their adaptability can bring significant insights to optimizing future wet adhesives.

References

1. Zhao H, Waite JH (2006) J Biol Chem 281(36):26150–26158
2. Zhao H et al (2006) J Biol Chem 281(16):11090–11096
3. Lee H, Scherer NF, Messersmith PB (2006) Proc Natl Acad Sci U S A 103(35):12999–13003

4. Lee H, Lee BP, Messersmith PB (2007) Nature 448(7151):338–341
5. Glass P et al (2009) Langmuir 25(12):6607–6612
6. Zhou WH et al (2010) J Mater Chem 20(5):880–883
7. Brubaker CE et al (2010) Biomaterials 31(3):420–427
8. Li SC et al (2010) Science 328(5980):882–884
9. Yamamoto H (1987) J Chem Soc Perkin Trans 1(3):613–618
10. Yu ME, Deming TJ (1998) Macromolecules 31(15):4739–4745
11. Ninan L et al (2007) Acta Biomater 3(5):687–694
12. Cha HJ et al (2009) Biofouling 25(2):99–107
13. Wang JJ et al (2008) Adv Mater 20(20):3872
14. Lin Q et al (2007) Proc Natl Acad Sci U S A 104(10):3782–3786
15. Hwang DS et al (2010) J Biol Chem 285(33):25850–25858
16. Tamarin A, Lewis P, Askey J (1976) J Morphol 149(2):199–221
17. Sagert J, Waite JH (2009) J Exp Biol 212(14):2224–2236
18. Freund J, Kalbitzer HR (1995) J Biomol NMR 5(3):321–322
19. Proudfoot GM, Ritchie IM (1983) Aust J Chem 36(5):885–894
20. Haemers S et al (2002) Langmuir 18(12):4903–4907
21. Rzepecki LM, Waite JH (1991) Arch Biochem Biophys 285(1):27–36
22. Liu B, Burdine L, Kodadek T (2006) J Am Chem Soc 128(47):15228–15235
23. Rzepecki LM, Nagafuchi T, Waite JH (1991) Arch Biochem Biophys 285(1):17–26
24. Michibata H et al (2003) Coord Chem Rev 237(1–2):41–51
25. Jensen KS, Hansen RE, Winther JR (2009) Antioxid Redox Signal 11(5):1047–1058
26. Brandes N, Schmitt S, Jakob U (2009) Antioxid Redox Signal 11(5):997–1014
27. Anderson TH et al (2010) Adv Funct Mater 20(23):4196–4205
28. Israelachvili JN (2011) Intermolecular and surface forces, 3rd edn. Academic, Burlington, MA
29. Inaba K (2010) Genes Cells 15(9):935–943
30. McDowell LM et al (1999) J Biol Chem 274(29):20293–20295
31. Zeng HB et al (2010) Proc Natl Acad Sci U S A 107(29):12850–12853
32. Depuydt M et al (2009) Science 326(5956):1109–1111
33. Ottaviano FG, Handy DE, Loscalzo J (2008) Circ J 72(1):1–16

Chapter 5
Hydrophobic Enhancement of Dopa-Mediated Adhesion in a Mussel Foot Protein

5.1 Introduction

The California mussel, *Mytilus californianus*, thrives in the exposed wave-swept habitats along the Pacific coast of North America, secured by its versatile, rapid, and permanent adhesion to diverse solid substrata. Given the hundreds of reports on mussel-inspired adhesives in recent years [1–6], investigations of the adhesion mechanism of *M. californianus* have had a profound impact on the design and production of man-made adhesives that work in a wet environment as well as spurring new approaches to prevent fouling which is of major economic concern to marine shipping [7], heat exchangers [8], and biomedical implants [9–11].

Mussel adhesion is mediated by a holdfast structure known as the byssus, essentially a bundle of leathery threads tipped by flat adhesive plaques that attach to a variety of hard surfaces (Fig. 5.1) [12]. At least nine proteins have been characterized from the adhesive plaques of Mytilus species and several of them are well characterized. Dopa is the prominent functionality in most Mfps (mussel foot proteins) that allows them to adhere to various surfaces underwater, as well as contributing to the cohesion within the plaques. Adhesive versatility is facilitated by Dopa's ability to form hydrogen bonds with hydrophilic surfaces (e.g., mica, hydroxyapatite) [13, 14] and participate in coordination bonding with metal ions and metal oxides, and undermined by Dopa's notorious susceptibility to oxidation [15]. For example, following the pH induced autoxidation of Dopa at neutral to basic pH, the adhesion of Dopa-rich Mfp-3 *fast* to a mica surface is almost completely abolished [13, 16]. Clearly there is little to be gained by adopting a Dopa-like chemistry in synthetic adhesive polymers if autoxidation cannot be controlled. Mussels stringently control Dopa oxidation, and a better understanding of their control mechanisms would help to engineer better biomimetic adhesives. In one known mechanism, antioxidant thiolates in Mfp-6 rescue Dopa in Mfp-3 and Mfp-5 from oxidized Dopaquinones [16].

J. Yu, *Adhesive Interactions of Mussel Foot Proteins*, Springer Theses,
DOI 10.1007/978-3-319-06031-6_5,

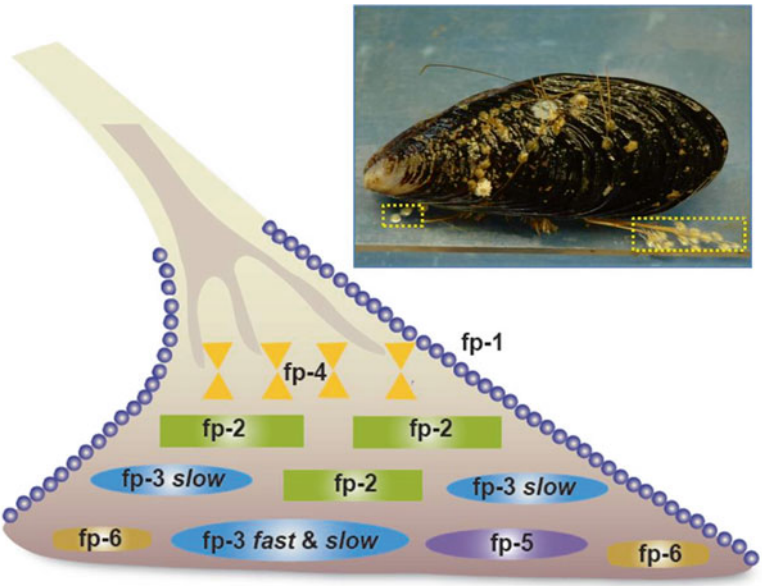

Fig. 5.1 Byssal plaque proteins of Mytilus. A mussel (*M. californianus*, *inset*) is shown attached to a polymer plate. One of its plaques (shown in *dotted yellow box*) is schematically enlarged to illustrate the approximate distribution of known proteins

In this chapter, I show that mussels have another strategy to improve the adhesive performance of Dopa at neutral pH. Nor is Dopa the only cohesive linker in mussel plaque; hydrophobic interaction and inter-residue H-bonding also play important roles. These important new insights are both observed in the Mfp-3 *slow* group of Mfp-3 variants. Dopa-rich Mfp-3 has about 30 different variants in the mussel plaque, which can be subdivided into two groups, Mfp-3 *fast and slow*. In previous studies, focus had been on the adhesion properties and performance of Mfp-3 *fast*, which was shown to be able to bridge two mica surfaces, acting like a molecular glue [13, 16, 17]. The other big family of the Mfp-3 variants, Mfp-3 *slow*, is less well understood [18]. The defining differences between Mfp-3 *fast* and Mfp-3 *slow* variants are that their eluting fractions in reverse phase HPLC are well separated as are their progress on acetic acid-urea polyacrylamide gel (AU-PAGE).

Both Mfp-3 *fast and slow* have low molecular weights with masses between 5 and 7 KDa. Compositionally (Fig. 5.2), Mfp-3 *slow* has much lower content of basic arginine and lysine; in Mfp-3 *fast*, almost all the tyrosine residues are post-translationally modified to Dopa (17–20 mol%), whereas in Mfp-3 *slow*, approximately half are modified (8–14 mol%). The lower charge density results in Mfp-3 *slow* being a very hydrophobic protein as seen in the hydropathy plot in Fig. 5.2c. Mfp-3 *slow* is the most abundant directly extractable protein from the byssus plaques of *M. californianus*, with a yield more than twice that of Mfp-3 *fast*. Based on a comparison of the tryptophan (Trp) content of Mfp-3 and whole plaque, it is estimated that the proportion of Mfp-3 *slow* in plaque to be at least 16 %.

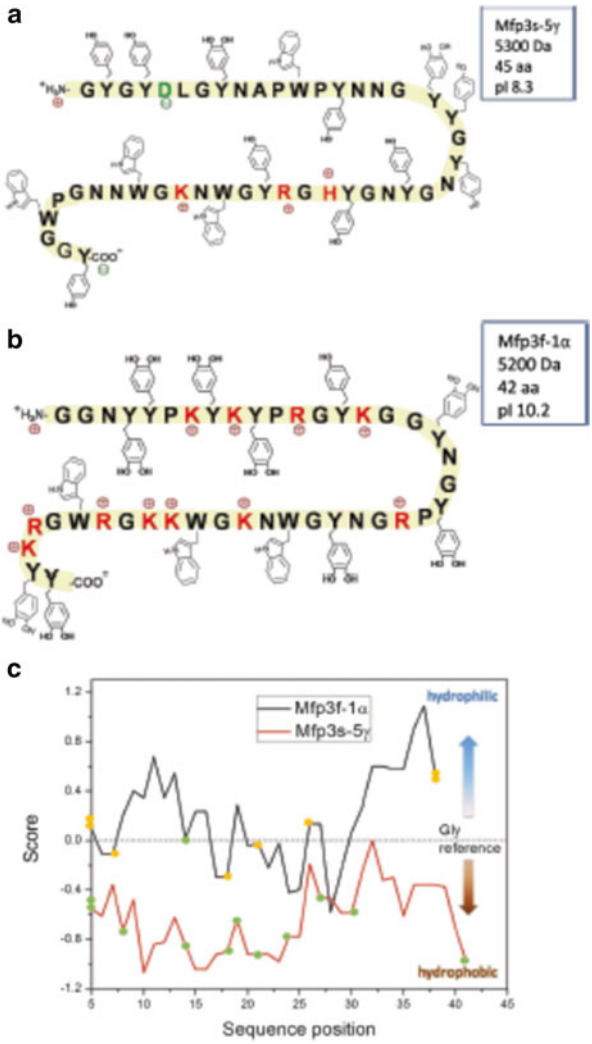

Fig. 5.2 Sequences of (**a**) Mcfp3-5γ and (**b**) Mfp-3-1α, with (**c**) their Hopp and Woods hydropathy (ExPaSy tools) plots using hydropathy values from Nozaki and Tanford [10] for standard amino acids and Dopa with window size 9 (*Orange spots* denote Dopa; *green spots* denote Tyr). The Dopa residues in the Mfp-3-5 sequence are unassigned and could occur wherever Tyr is present

In this chapter, the adhesion of Mfp-3 *slow* to mica, the self-interactions between Mfp-3 *slow* layers, and the interactions between Mfp-3 *slow* and other proteins (Mfp-3 *fast* and Mfp-2) were tested using a surface forces apparatus (SFA). The SFA has proven to be a suitable and powerful technique for studying protein adhesion [12, 17, 20–22]. The present SFA studies demonstrate that Mfp-3 *slow* binds to mica surfaces and exhibits significant cohesion between two Mfp-3 *slow* layers over a wide range of pH (from 3 to 7.5). Interchain and inter-residue hydrogen-bonding characteristic of secondary structure, together with hydrophobic interaction, could be the main sources of Mfp-3 *slow* cohesion at pH 5.5 and 7.5.

5.2 SFA Measurement

The interactions between the Mfp-3 *slow* films and an Mfp-3 *slow* film with another Mfp film were measured by an SFA 2000. The protein deposition was done by placing 20 μL of Mfp-3 *slow* solution (20 μg/mL) together with 100 μL of pH 3 buffer onto one or both mica surfaces. After 30 min absorption followed by rinsing with buffer with the desired pH, the two surfaces were mounted in the SFA chamber with a droplet of buffer (~100 μL) sandwiched in between for measurement. All experiments were performed at a controlled room temperature (22 °C). To adjust the pH of protein solution droplets on mica surfaces, the following stock buffers were used for rinsing: 0.1 M sodium acetate (EM Science, Gibbstown, NJ) and 0.25 M potassium nitrate titrated by acetic acid (pH 5.5); 0.016 M potassium phosphate monobasic (Mallinckrodt, Hazelwood, MO), 0.084 M potassium phosphate dibasic (EMD Chemicals, Gibbstown, NJ), and 0.25 M potassium nitrate (pH 7.5). Milli-Q water (Millipore, Bedford, MA) was used for all the glassware cleaning and solution preparation.

5.3 The Adhesive Properties of Mfp-3 *Slow* on Mica

The adhesive properties of Mfp-3 *slow* on mica surfaces were investigated by SFA at three different pHs (Fig. 5.3a). The SFA provides a precise and sensitive means of quantifying the interaction forces between polymers or between polymers and surfaces. Mica is atomically smooth and biologically relevant (cf. clay-based rocks) as a support/substrate surface onto which various Mfps can be adsorbed and their interactions examined at appropriate solution conditions (salinities, pH, temperatures, etc.) [16].

The interaction between one Mfp-3 *slow* coated and another bare mica surface was measured as a function of surface separation distance at pH 3 (Fig. 5.3b). During the approach, the first observable interaction was the "steric" repulsion caused by the entropic confinement of proteins. The surfaces were further compressed until the distance between two surfaces reached a constant value (the "hard wall"). After a short holding period (~3 min), the surfaces were separated and an adhesion energy of $E_{ad} \sim -0.95$ mJ/m^2 when the surfaces "jumped" apart. When the same experiment was repeated at pH 5.5 and 7.5, the adhesion energy decreased to −0.42 mJ/m^2 and −0.32 mJ/m^2, respectively (Fig. 5.3c, d).

These results showed that, similar to the fast Mfp-3 variants, an Mfp-3 *slow* film is also capable of adhering well to a bare mica surface (asymmetric configuration). Given that the Dopa-rich Mfp-to-mica interaction is attributed to hydrogen bonds (H-bonds) between the bidentate OH groups of the catecholic side groups and the O atoms in the mica polysiloxane lattice [13, 16] and that on average Mfp-3 *slow*

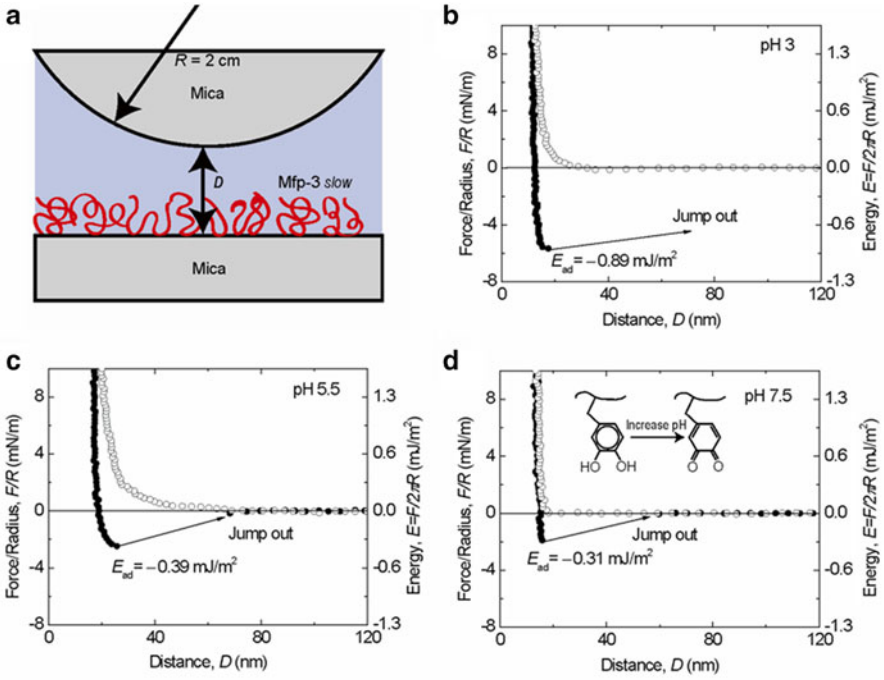

Fig. 5.3 Interaction between mica and Mfp-3 *slow* adsorbed to mica at pH 3 (**b**), 5.5 (**c**), 7.5 The experimental geometry is show in (**a**). (**d**). The *y* axis on the left gives the measured force, *F*/*R* (normalized by the radius of the surface), whereas the *y* axis on the right gives the corresponding adhesion energy *E* per unit area between two flat surfaces, defined by $E = F/2\pi R$. Approach (*unfilled symbols*); separation (*unfilled symbols*). Separation followed a brief (~3–5 min) contact. The interaction between Dopa and mica is H-bonding, which decreases as pH increases due to Dopa oxidation

has half as much Dopa as Mfp-3 *fast*, it is reasonable to expect weaker adhesion for Mfp-3 *slow* to mica ($E_{ad} \sim -0.95$ mJ/m^2) at pH 3 than for Mfp-3 *fast* ($E_{ad} \sim -2$ mJ/m^2). The trend of decreased adhesion with increasing pH (Fig. 5.3d) also parallels what was previously observed for Mfp-3 *fast* [13]. However, at pH 7.5, the adhesion of Mfp-3 *slow* is still significant, being about 1/3 of that measured at pH 3, whereas for Mfp-3 *fast* no adhesion was measurable at pH 7.5. This discrepancy suggests that Dopa residues in the two protein variants (Mfp-3 *fast* and *slow*) may be differentially prone to oxidation at the same pH. To verify that Dopa is essential for Dopa/mica bonding, Dopa of Mfp-3 *slow* in the asymmetric configuration was periodate oxidized. Following periodate addition, the adhesion was abolished (Fig. 5.4), which suggests Mfp-3 *slow* with oxidized Dopa cannot adhere to mica.

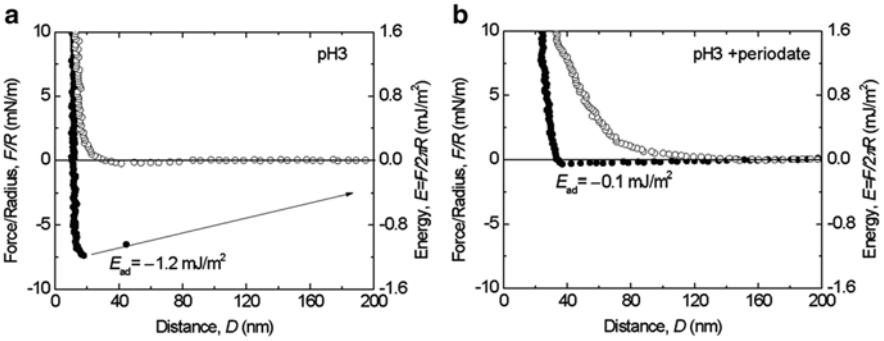

Fig. 5.4 Interaction between mica and Mfp-3 *slow* adsorbed on mica at pH 3 (**a**) before and (**b**) after adding excess $NaIO_4$

5.4 The Cohesion (Self-Interaction) of Mfp-3 *Slow*

The self-interaction or cohesion of Mfp-3 *slow* layers was measured using a symmetric configuration, i.e., having Mfp-3 *slow* films on both mica surfaces (Fig. 5.5). At pH 3, moderately strong adhesion of $E_{ad} \sim -1.8$ mJ/m^2 (Fig. 5.5b) was measured on separating the surfaces. Surprisingly, the adhesion forces measured at higher pHs did not exhibit a significant pH dependence. The strong adhesion forces persisted, with adhesion energies of −1.8 mJ/m^2 and −1.4 mJ/m^2, respectively, (Fig. 5.5c, d) at the two higher pHs studied (pH 5.5 and 7.5). At all three pH conditions, a longer contact time prior to separation resulted in a stronger interaction. In particular, after the two surfaces were in contact for 65 min, Mfp-3 *slow* showed even higher interaction energies at pH 5.5 (−3.7 mJ/m^2) and 7.5 (−3.0 mJ/m^2) compared with that at pH 3 (−2.9 mJ/m^2). The ability to maintain strong interactions at pH 5.5 and 7.5 distinguishes Mfp-3 *slow* cohesive self-interactions from those of both Mfp-3 *fast* and *slow* on mica surfaces. In the asymmetric configuration experiments, the adhesion strength—attributed to the formation of H-bonds between Dopa residues in Mfp-3 *slow* and mica—dropped as pH-dependent Dopa autoxidation increased. Does the Dopa oxidation associated with increased pH also diminish the cohesive interactions in the Mfp-3 *slow* symmetric experiment? Clearly, it does not (Fig. 5.5). Cohesion between Mfp-3 *slow* layers remains as strong at pH 5.5 and 7.5 as at pH 3, thereby suggesting that other interactions are contributing.

As mentioned earlier, at least 60 % of the amino acid residues in the sequence of Mfp-3 *slow* are more hydrophobic than glycine. The pI values of Mfp-3 *slow* variants range from 8 to 9. Indeed, as the pH approaches the protein pI, the electrostatic repulsion between two symmetric protein surfaces is eliminated leading to enhanced hydrophobic interactions. Hydrophobic interactions may thus account for the strong cohesion between symmetric Mfp-3 *slow* films when the pH increases from 3 to 5.5 then 7.5.

Excess periodate was also introduced between the mica surfaces with symmetrically deposited Mfp-3 *slow* at pH 3. Almost no attractive interaction (adhesion) and

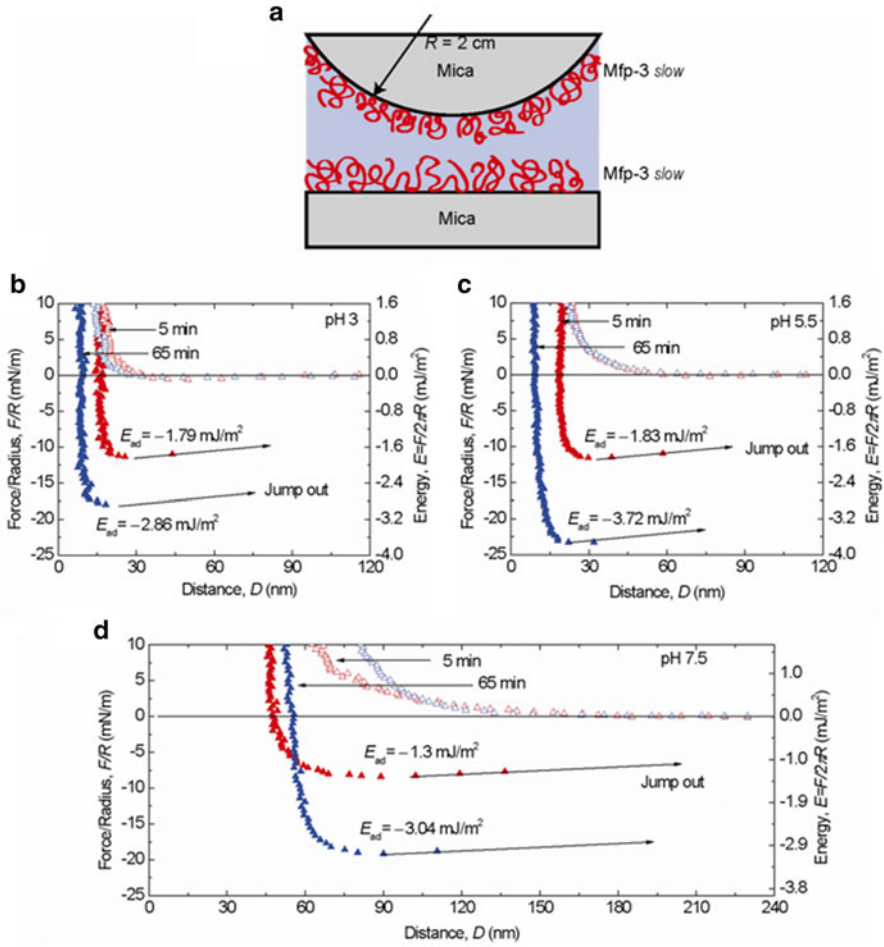

Fig. 5.5 Interaction between Mfp-3 *slow* layers absorbed onto mica at (**b**) pH 3; (**c**) pH 5.5; (**d**) pH 7.5. Contact times were as shown. Approach (*unfilled symbols*); separation (*unfilled symbols*). The experimental geometry is shown in (**a**)

a threefold greater hardwall (repulsion) occurred (Fig. 5.6). One interpretation of this result is that if the hydrophobic contribution to the protein–protein interaction remains high, the interface between Mfp-3 *slow* and mica becomes the weak link. However, the measured E_{ad} of the asymmetrically deposited Mfp-3 *slow* at pH 3 was −0.89 mJ/m^2 (Fig. 5.3), less than half that for the symmetric configuration (E_{ad} = −2.3 mJ/m^2 Fig. 5.6); hence it is not clear that that the Mfp-3-mica interface became the new weak link. Moreover, the Dopa already bound to the polysiloxane mica surface should not be readily available to periodate oxidation unless the Dopa-periodate complex formed is more stable. Periodate must form a bidentate chelate with the catecholic moiety of Dopa in order to oxidize it [24].

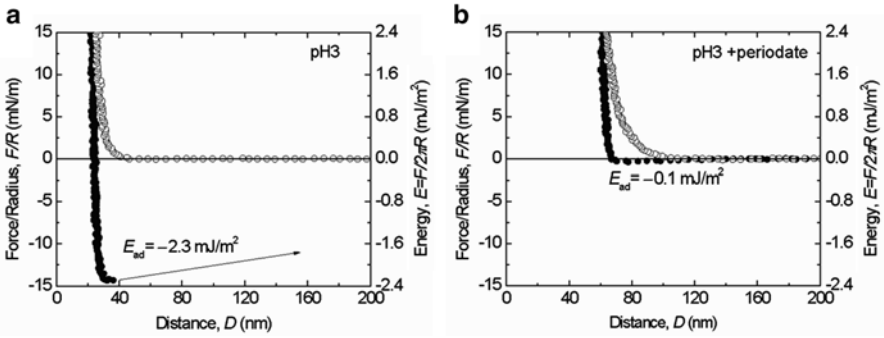

Fig. 5.6 Interaction measured at pH 3 between two mica surfaces with Mfp-3 *slow* absorbed symmetrically (**a**) before and (**b**) after adding excess amount $NaIO_4$

5.5 ATR-FTIR Measurement

H-bonding is an important interaction that is abundantly common within a protein molecule as well as between different molecules; it also stabilizes protein secondary structure. Correspondingly, secondary structure in proteins could be an indication of H-bonding between chains or side groups. In order to determine if Mfp-3 *slow* structure changes with pH, FTIR spectra of Mfp-3 *slow* were taken at pD 3, 5.5, and 7.5 in deuterated acetate or phosphate-buffered saline (Fig. 5.7). The results are shown in Fig. 5.6. The primary peak for pD 3 was at 1,643 cm^{-1}, which can be assigned to a random coil secondary structure.

At both pD 5.5 and 7.5, the proteins phase-separate from the solvent, some of which is deposited on the surface of ATR crystal forming a patchy hydrated layer. ATR-FTIR spectra at both pDs showed that Mfp-3 *slow* has an ordered secondary structure at these higher pD regimes compared with the random coil configuration under pD 3 conditions.

Significant differences in the amide I′ peak were observed in the pD 5.5 spectrum compared to that of pD 3: notably, there was a complete loss of the random coil signature (1,643 cm^{-1}) and the appearance of new bands at 1,632, 1,652, 1,669, and 1,682 cm^{-1}. The prominent peak at 1,632 cm^{-1} and smaller peak at 1,682 cm^{-1} are both associated with β sheets. The peak at 1,669 cm^{-1} is generally assigned to reverse turns [23, 25–28]. The 1,652 cm^{-1} peak indicates the presence of α-helices. Upon further increasing pD value to 7.5, a slight shift of low frequency β sheet from 1,632 to 1,630 cm^{-1} was observed, together with a smaller peak at 1,661 cm^{-1} which is associated with both α-helices and extended turns [21]. A shift was also observed for the high frequency β-sheet feature at 1,677 cm^{-1} (1,682 cm^{-1} for pD 5.5).

To summarize, as pD was increased from 3 to 5.5, Mfp-3 *slow* transformed from a random coil to highly ordered structure, which consists mostly of β sheet and turns mixed with some α-helices. At pD 7.5, β sheet and turns prevail as well, accompanied by α-helices and random coils. The random structure of soluble Mfp-3 *slow* at

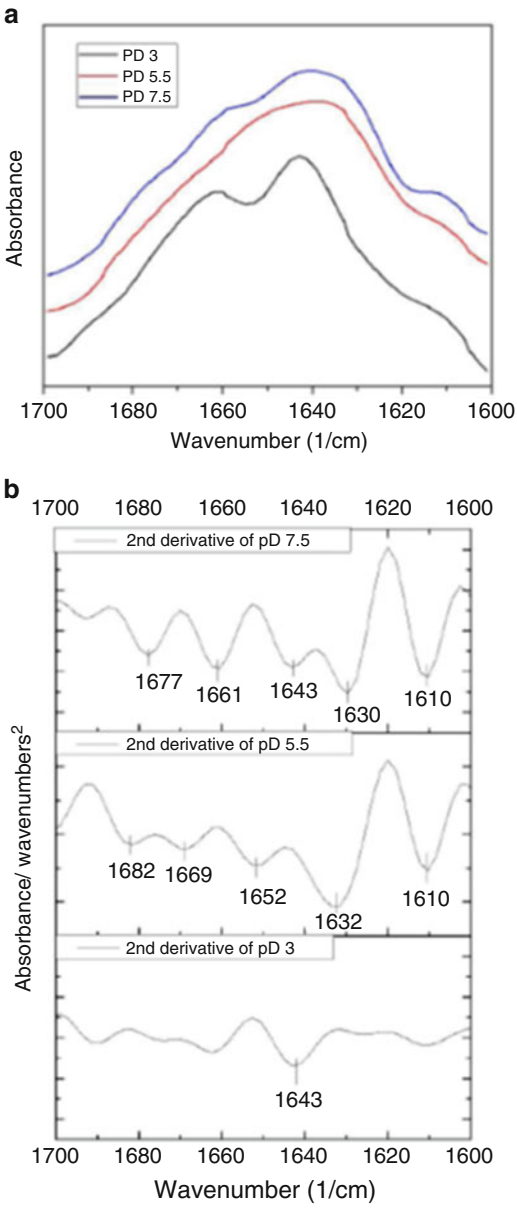

Fig. 5.7 ATR-FRIR Spectra of Mfp-3 *slow* at different pD. (**a**) ATR-FTIR spectra of 0.5 mg/mL Mfp-3 *slow* in deuterated buffers at three different pH conditions used for SFA experiments. The signal of pD 3 and 7.5 were magnified 20 and 5 times respectively for the convenience of comparison. (**b**) Second derivative of spectra (**a**): The primary peak at pD 3 at 1,643 cm^{-1} can be assigned to random coils. At pD 5.5, The prominent peak 1,632 cm^{-1} is associated with β sheet, and 1,682 cm^{-1} with high β sheet. Band at 1,669 cm^{-1} is generally assigned to turns. Peak at 1,652 cm^{-1} indicates the existence of α-helices. At pD 7.5, low β sheet slightly shifted to 1,630 cm^{-1} was observed. Peak at 1,661 cm^{-1} can be associated with both α-helices and extended turns. A shift was also observed for the high frequency β-sheet feature at 1,677 cm^{-1}

pH 3 was confirmed by CD spectroscopy (Fig. 5.7). CD measurements at the other two pH conditions were not possible as the phase-separated proteins tended to scatter light. According to ATR-FTIR results, H-bonds contribute more to protein secondary structure at pH 5.5 and 7.5 than at pH 3.

5.6 Discussion

Dopa has emerged as a crucial component for achieving both adhesion of protein to various surfaces and for cohesion between mussel adhesive proteins. As a result, diverse synthetic systems have been engineered with Dopa to provide wet adhesion. However, in a number of synthetic polymers and purified adhesive proteins, adhesion failure on various substrates due to Dopa oxidation is well known, especially at neutral to basic pH. The decrease of adhesion to mica with increasing pH from 3 to 5.5 then 7.5 was also observed for Mfp-3 *slow* but was less pronounced than its electrophoretically fast variant. For example, almost no adhesion was measured at pH 7.5 for Mfp-3 *fast*, whereas 1/3 of the adhesion energy at pH 3 still remained for Mfp-3 *slow*.

Mfp-3 *slow* is the most hydrophobic protein in mussel plaques. At pH 7.5, which is close to its pI, the Mfp-3 *slow* protein molecules will therefore tend to pack more closely due to the absence of electrostatic repulsion and (likely enhanced) hydrophobic interaction. It is likely that the Dopa residues in Mfp-3 *slow* are nested in a hydrophobic microenvironment, which prevents them from being naturally exposed to the surrounding aqueous environment. As such, the measured redox potential of Mfp-3 *slow* is higher than that of Mfp-3 *fast*. This could also explain why in the SFA data, the loss of Dopa/mica hydrogen-bonding interaction in Mfp-3 *slow* is much less than in Mfp-3 *fast* when the pH is raised from fairly acidic to slightly basic.

For practical adhesive bonding, cohesion within the adhesive is as important as the interfacial adhesion. For marine mussels, while the interfacial adhesion between plaques and various surfaces influences how strongly mussel adhesive proteins bind to surfaces, they also need strong cohesive interactions to maintain the integrity of their byssal plaques and threads. Till now, two Mfps have been shown to contribute to the cohesive strength of mussel plaques by SFA measurements in which proteins are deposited on both surfaces: Mfp1 forms Dopa-Fe^{3+} coordination complexes, which increase both the stiffness and hardness of the plaque cuticle [29, 30]; Mfp-2 binds to Mfp-5 at the interface and to other Mfp-2 in the presence of Ca^{2+} and Fe^{3+} in the plaque, functioning as a bridge between the plaque interface and the scaffolding collagens and associated matrix proteins that join the thread to the plaque [31]. From these two cases, Dopa/metal ion coordination is the mechanism that can be extracted for translation into synthetic systems. My studies have shown that Mfp-3 *slow* is also an important participant in the cohesion of mussel plaque, which is not mediated by metal ions. Given the strong cohesive interaction shown over the pH range of 3–7.5, it is unreasonable to attribute the interaction to Dopa/Dopa or Dopa/residues H-bonding completely, which should diminish with increasing pH.

The hydrophobic interaction, a long-range interaction, is significant to protein function in terms of driving protein folding and self-assembly in biomacromolecules [32–34]. But its importance in wet adhesion has barely been investigated [35] especially in the sense of reinforcing the self-self protein interactions. Considering the high content of amino acids with hydrophobic side chains in Mfp-3 *slow*, it is reasonable to conclude claim that inter- and intramolecular hydrophobic interactions are playing a role in the impressive cohesion measured by SFA. But at this

point, it is still unclear how pH affects the hydrophobic interaction [36]; thus I am not able quantify the contribution of the hydrophobic interaction to protein cohesion in these measured conditions. Secondary structure transformation of Mfp-3 *slow* suggested by FTIR results indicates the development of inter-residue H-bonding when switching the pH from 3 to 5.5 and 7.5. As the pH approaches the pI, the elimination of the electrostatic repulsion between protein molecules and enhanced hydrophobic interaction leads the proteins to assemble and enables the occurrence of local H-bonding. Based on these analyses, the strong hydrophobic character of Mfp-3 *slow* is a key factor for increasing cohesion within layers.

5.7 Conclusion

I have shown that Dopa nested in hydrophobic aromatic sequences not only enhances adhesion at neutral pH (pI or IEP) but also contributes significantly to the cohesive interactions between adhesive proteins. The high proportion of hydrophobic amino acid residues in Mfp-3 *slow* sequence provides Dopa with a microenvironment that retards oxidation by shielding the amino acids from the solvent and endows the protein with the ability to maintain adhesion at slightly basic pH.

More importantly, hydrophobic interactions and inter-residue H-bonding combine to result in strong cohesion within Mfp-3 *slow* layers over a relatively wide range of pH. This strategy provides an alternative to Dopa/metal ion chelation and compensates in part for limitations imposed by facile Dopa autoxidation. By exploring the adhesive and cohesive mechanisms of bonding by Mfp-3 *slow*, these studies reveal that the wet adhesion of mussels is more complicated than a simple Dopa-mediated recipe and provide a rationale for engineering Dopa into a new generation of bio-inspired synthetic adhesive polymers.

References

1. Lee H et al (2007) Science 318(5849):426–430
2. Lee H, Lee BP, Messersmith PB (2007) Nature 448(7151):338–341
3. Lee YH et al (2008) Adv Mater 20(21):4154
4. Ham HO et al (2011) Angew Chem Int Ed 50(3):732–736
5. Westwood G, Horton TN, Wilker JJ (2007) Macromolecules 40(11):3960–3964
6. Matos-Perez CR et al (2011) Abstr Paper Am Chem Soc 241
7. Anderson C et al (2003) J Mar Des Oper B4:23
8. Cho YI, Choi BG (1999) Int J Heat Mass Tran 42(8):1491–1499
9. Ratner BD (1993) J Biomed Mater Res 27(7):837–850
10. Wisniewski N, Reichert M (2000) Colloids Surf B Biointerfaces 18(3–4):197–219
11. Bryers JD (1994) Colloids Surf B Biointerfaces 2(1–3):9–23
12. Waite JH et al (2005) J Adhes 81(3–4):297–317
13. Yu J et al (2011) Adv Mater 23(20):2362
14. Chirdon WM, O'Brien WJ, Robertson RE (2003) J Biomed Mater Res B Appl Biomater 66B(2):532–538

15. Lee H, Scherer NF, Messersmith PB (2006) Proc Natl Acad Sci U S A 103(35):12999–13003
16. Yu J et al (2011) Nat Chem Biol 7(9):588–590
17. Lin Q et al (2007) Proc Natl Acad Sci U S A 104(10):3782–3786
18. Zhao H et al (2006) J Biol Chem 281(16):11090–11096
19. Nozaki Y, Tanford C (1971) J Biol Chem 246(7):2211
20. Israelachvili JN, Adams GE (1978) J Chem Soc Faraday Trans I 74:975
21. McGuiggan PM, Israelachvili JN (1990) J Mater Res 5(10):2232–2243
22. Israelachvili JN (2011) Intermolecular and surface forces, 3rd edn. Academic, Burlington, MA
23. Byler DM, Susi H (1986) Biopolymers 25(3):469–487
24. Weidman SW, Kaiser ET (1966) J Am Chem Soc 88(24):5820
25. Goormaghtigh E, Cabiaux V, Ruysschaert JM (1990) Eur J Biochem 193(2):409–420
26. Zurdo J, Guijarro JI, Dobson CM (2001) J Am Chem Soc 123(33):8141–8142
27. Torrent J et al (2004) Biochemistry 43(22):7162–7170
28. Serrano V, Liu W, Franzen S (2007) Biophys J 93(7):2429–2435
29. Harrington MJ et al (2010) Science 328(5975):216–220
30. Zeng HB et al (2010) Proc Natl Acad Sci U S A 107(29):12850–12853
31. Hwang DS et al (2010) J Biol Chem 285(33):25850–25858
32. Dill KA (1999) Protein Sci 8(6):1166–1180
33. Dill KA (1990) Biochemistry 29(31):7133–7155
34. Ghosh K, Dill KA (2009) J Am Chem Soc 131(6):2306–2312
35. Kamino K, Nakano M, Kanai S (2012) FEBS J 279(10):1750–1760
36. Meyer EE, Rosenberg KJ, Israelachvili J (2006) Proc Natl Acad Sci U S A 103(43): 15739–15746

Chapter 6
Learning from the Pieces: The Adhesion of Mussel-Inspired Peptides

6.1 Introduction

Marine mussels have an extraordinary ability to achieve and maintain strong wet adhesion that relies on adhesive proteins rich in 3,4-L-dihydroxyphenylalanine (Dopa). Dopa forms bidentate coordination complexes with many metal oxide surfaces and multivalent cations in solution [1–5], hydrogen bonds with many hydrophilic surfaces [6–11] and, when oxidized, covalent cross-links with biomacromolecules [12, 13]. Of the ten known mussel foot proteins (Mfps), Mfp-5 has the highest Dopa content and exhibits the strongest adhesion energy on mica substrates [6, 14, 15]. Given these distinctions, Mfp-5 has become an attractive molecular paradigm for mimicking mussel adhesion and has inspired numerous investigations of Dopa- or catechol-functionalized synthetic materials for various applications including wet adhesives [13, 16–20], antifouling coatings [21, 22], magnetic imaging agents [23], tissue glues [24], and pH-sensitive hydrogels [3]. Although several reports have emphasized the importance of Dopa in mussel protein adhesion, due to the large size and complexity of the Mfp molecules, significant details remain unclear [10, 11, 22]. Two persistent questions are as follows: (1) How do the flanking amino acid sequences effect Dopa adhesion? (2) How do interactions besides those involving Dopa help to mediate the adhesion of Mfps [25]? To answer these questions, we prepared three short, Mfp-5-derived synthetic peptides 15–16 residues in length with and without enzymatic modification of tyrosine (Y* denotes tyr to Dopa): VGSGY*DGY*SDGY*Y*DG (PEP pI 4), HY*HSGGSY*HGSGY*- -HG (PEP pI 6.5), and GY*KGKY*Y*GKG KKY*Y*Y*K (PEP pI 10) (Figs. 6.1 and 6.2). The repulsive and attractive forces of these peptides on mica surfaces were investigated with an SFA 2000.

J. Yu, *Adhesive Interactions of Mussel Foot Proteins*, Springer Theses,
DOI 10.1007/978-3-319-06031-6_6,

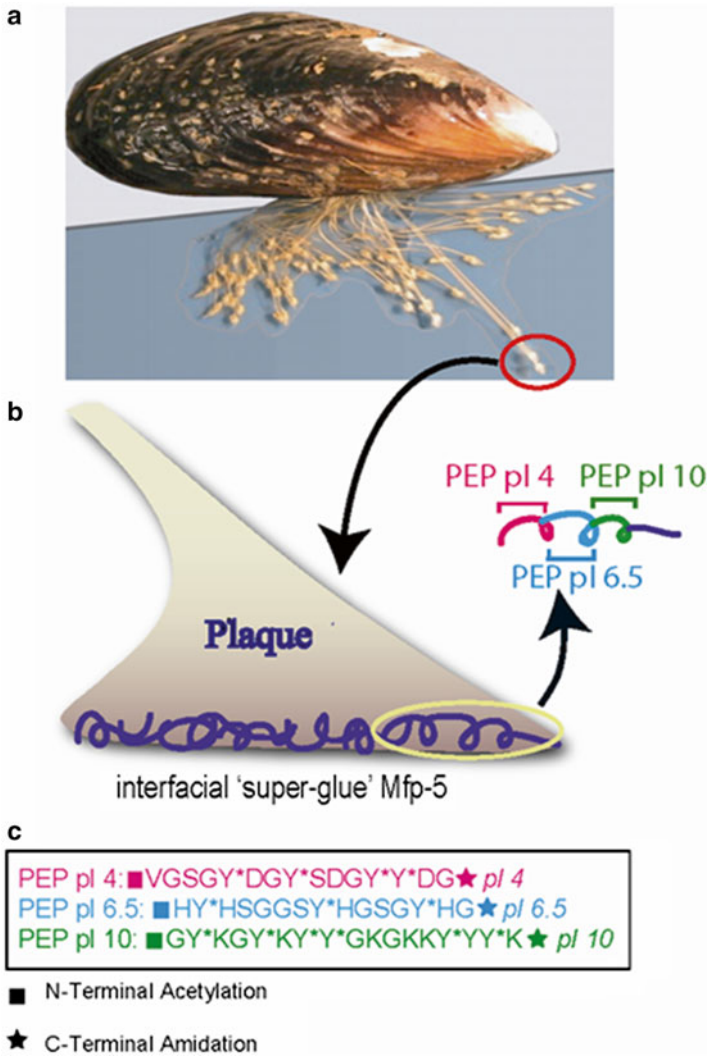

Fig. 6.1 (**a**) An adult mussel attached to a glass surface by a byssus containing many threads and adhesive plaques. (**b**) Schematic zoom of a plaque, showing the "super glue" Mfp-5 at the plaque interface. (**c**) Three unique sequences with 15–16 amino acid residues were selected from the Mfp-5 sequence. All three peptides have different pIs

6.2 Enzymatic Modification of the Peptides

Here, a mushroom tyrosinase was used to o-hydroxylate peptidyl tyr to Dopa (Fig. 6.3a), but this enzymatic conversion requires safeguards to reduce the formation of undesirable side products such as 3,4,5-trihydroxyphenylalanine (Topa) and

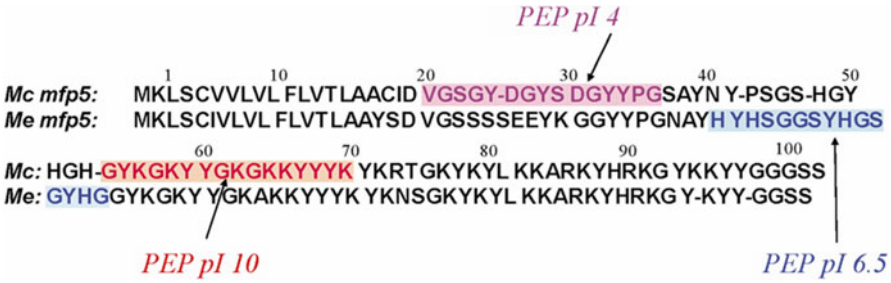

Fig. 6.2 Aligned sequences of Mfp-5 from *Mytilus californianus* (Mc) and *Mytilus edulis* (Me) showing the locations of synthetic PEP pI 4, PEP pI 6.5, and PEP pI 10. Whereas PEP pI 10 is nearly the same in both species, the others show degrees of difference. Although the sequence of PEP pI 4 is acidic in both, the Mc sequence was preferred as the basis of the synthetic VGSGYDGYSDGYYDG because serines in the Me cluster (S23–S26) are known to be phosphorylated. PEP pI 6.5 was synthesized based on the Me sequence because with more histidine residues, its pI is better defined

Dopaquinone (Fig. 6.3b) [26]. By reversibly capturing Dopa immediately after it has formed, borate significantly improves Dopa yield and decreases side reactions. After stopping the reaction, modified peptides were separated by reverse-phase HPLC, which typically revealed three types of modified peptides, i.e., those that were (a) partially modified (some tyr residues are not modified), (b) completely modified (every tyr residue is modified), or (c) hypermodified (one or more tyr residues are converted to Topa) peptides. Electrospray ionization mass spectrometry (ESI) was used to measure the peptide masses in the eluting fractions. Those fractions with masses matching the calculated mass of completely modified (type b) peptides were pooled for amino acid analysis and sequencing by tandem MS (Fig. 6.3d). Amino acid analysis results (Fig. 6.3c) demonstrate that the compositions of pure modified PEP pI 4 and PEP pI 6.5 are consistent with calculated masses: Only traces of tyr remained, and no Topa was detectable. For PEP pI 10, there is persistently one tyr that eludes conversion to Dopa: This is Y-14, the central member in the Y-triad. Contact between tyrosinase and Y-14 is presumably impeded by the bulky borate groups on Y*-13 and Y*-15 during the modification.

6.3 The Adhesion Properties of the Peptides

The adhesion forces of modified peptides PEP pI 4, PEP pI 6.5, and PEP pI 10 on mica surfaces were measured using an SFA 2000. Prior to each experiment, 10 μL of peptide solution was added on top of one mica surface, letting the peptide adsorb on mica for 20 min followed by rinsing excessively with the same buffer to remove the non-adsorbed peptide molecules. All three peptides adhered to mica surfaces, with the strongest adhesion force, −4 mN/m (corresponding to a work of adhesion of 0.7 mJ/m^2), exhibited by PEP pI 10. PEP pI 6.5, although having the lowest Dopa

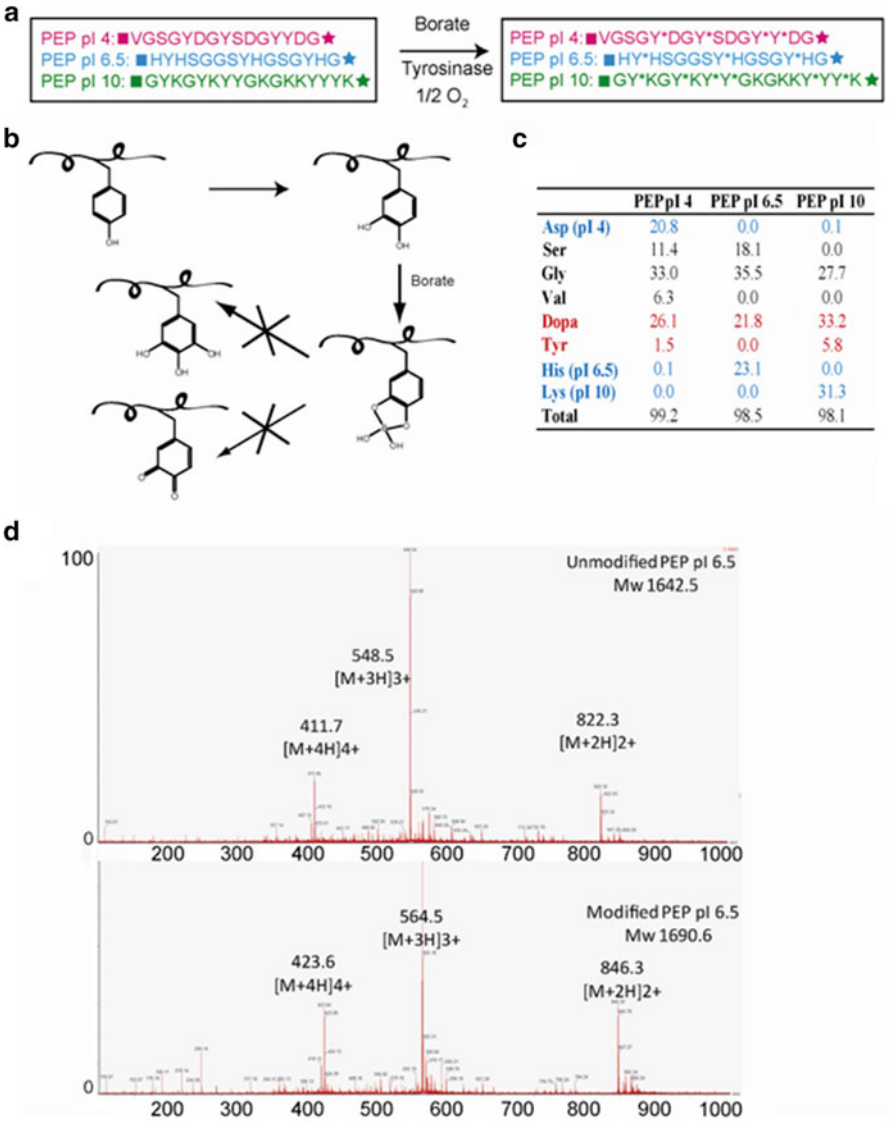

	PEP pI 4	PEP pI 6.5	PEP pI 10
Asp (pI 4)	20.8	0.0	0.1
Ser	11.4	18.1	0.0
Gly	33.0	35.5	27.7
Val	6.3	0.0	0.0
Dopa	26.1	21.8	33.2
Tyr	1.5	0.0	5.8
His (pI 6.5)	0.1	23.1	0.0
Lys (pI 10)	0.0	0.0	31.3
Total	99.2	98.5	98.1

Fig. 6.3 (**a**) The tyrosine residues in three peptides are enzymatically hydroxylated to Dopa. (**b**) Mushroom tyrosinase action is not limited to hydroxylation but further converts Dopa to Dopaquinone or Topa. To avoid these reaction products, borate is added to the solution to capture Dopa by formation of a reversible borate-Dopa chelate. (**c**) Amino acid analysis of the modified peptides after complete hydrolysis. (**d**) ESI results of PEP pI 6.5 before and after modification. Mass differences confirm that tyrosinase has introduced three hydroxylations to PEP pI 6.5 and the detection of Dopa by amino acid analysis confirm tyr as the modified target

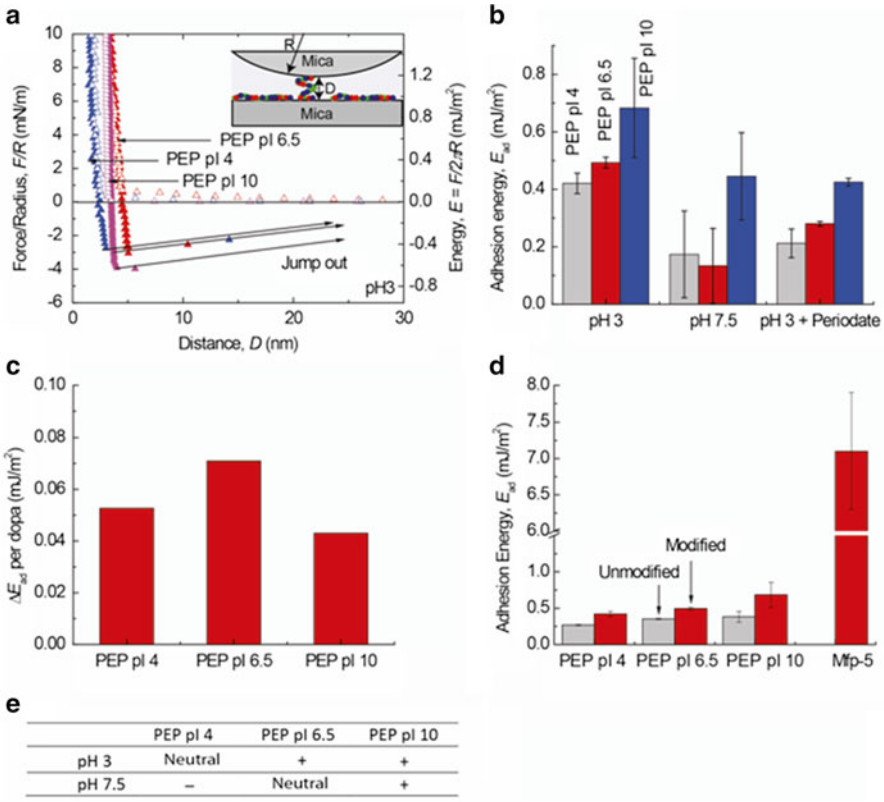

Fig. 6.4 (**a**) The force profiles of three peptides on mica surfaces. (**b**) A summary of adhesion energy of three peptides measured in pH 3, pH 7.5, and pH 3 with sodium periodate buffers. (**c**) The differences in E_{ad} per Dopa for three peptides before and after Dopa oxidation by periodate at pH 3. (**d**) A comparison of the adhesion energy of three peptides with and without tyrosinase modification and Mfp-5. The adhesion energies of three peptides shown in (**b**) and (**d**) are averaged from between 6 and 12 repetitive force runs from 2 to 4 different experiments at each treatment. Mfp-5 data are from [8]. (**e**) The charges (positive or negative) of three peptides in pH 3 and pH 7.5 buffers, respectively

content (only 3 Dopa out of 15 residues), exhibited an intermediate adhesion force of −3.0 mN/m, whereas the weakest adhesion force (−2.6 mN/m) belongs to PEP pI 4 (Fig. 6.4a). SFA results also demonstrate that Dopa plays an essential role in the adhesion of the peptides on mica surfaces. All three peptides adhered most strongly to mica surfaces at pH 3, at which Dopa is stable. Increasing the solution pH to 7.5, however, significantly reduced the adhesion. The work of adhesion dropped by 80 %, 60 %, and 35 % for PEP pI 6.5, PEP pI 4, and PEP pI 10, respectively (Fig. 6.4b). Given the different pIs of the three peptides, this drop of adhesion could be due to two possible reasons: (1) Dopa oxidation at high pH and (2) change of electrostatic interactions. Previous tests on mussel proteins [6, 10, 11] have shown

that Dopa undergoes autoxidation at pH 7.5, leading to diminished Mfp adhesion. Given their derivation from Mfp-5 sequences, the Dopa-containing peptides should be prone to similar oxidation tendencies. Dopa oxidation, however, does not explain why the pH affects the three peptides so differently.

6.4 Electrostatic Interactions Between the Peptides and Mica

Increasing pH also significantly changes the charge densities or the overall charge in three peptides. At pH 3, PEP pI 6.5 and PEP pI 10 are both positively charged, and both can interact with negatively charged mica surfaces through attractive electrostatic interactions [27]. Increasing the solution pH to 7.5 neutralizes the charges in PEP pI 6.5; therefore PEP pI 6.5 loses both the hydrogen bond of Dopa to mica surface (due to oxidation) and the attractive electrostatic interaction (histidine deprotonation), which results in the biggest drop in terms of the percentage of the adhesion force. In comparison, the sign and density of the charges in PEP pI 10 remain unchanged at pH 7.5, which enable PEP pI 10 to maintain attractive interactions between two mica surfaces despite depletion of Dopa by oxidation. Increasing pH also turns PEP pI 4 from a neutral to negatively charged molecule, thereby enhancing the electrostatic repulsion between PEP pI 4 and mica. The overall interaction, between mica and PEP pI 4, however, is still adhesive. The remaining adhesion force of PEP pI 4 after Dopa oxidation suggests other interactions involved in the peptide adhesion mechanism, possibly van der Waals force or hydrogen bonding from other hydrophilic groups in the peptide sequence, such as the serines.

The importance of electrostatic interactions is corroborated by injecting periodate, an artificial oxidant, into the solution between two mica surfaces at pH 3: The adhesion force of PEP pI 6.5 and PEP pI 4 both decreased by increasing the solution pH to 7.5 but to different degrees; in contrast to PEP pI 10, PEP pI 6.5 and PEP pI 4 both exhibited similar reduced attractive forces. The work of adhesion in PEP pI 6.5 at pH 3 is 0.28 mJ/m^2, almost three times the value measured at pH 7.5 (0.1 mJ/m^2). The increase of adhesion force by PEP pI 4 after oxidation by periodate at pH 3 compared with pH-dependent oxidation at 7.5 also strengthens our hypothesis about the involvement of electrostatic interactions in the binding of peptides to mica surfaces (Fig. 6.4b).

To further resolve the contributions of charged groups and Dopa in the adhesion of three peptides, I performed SFA tests on the unmodified peptides (no tyrosines converted to Dopa). All unmodified peptides showed similar work of adhesion to mica surface (0.27 ~ 0.35 mJ/m^2 Fig. 6.3c). Converting tyrosine to Dopa as much as doubled the adhesion energies of three peptides on mica surface, which confirms the importance of Dopa for the bridging adhesion of all the peptides. After oxidizing the Dopa group in the peptides by adding sodium periodate, the adhesion energies of three modified peptides dropped to values close to the unmodified peptides, also indicating the effect of enzymatic modification (Figs. 6.5 and 6.6).

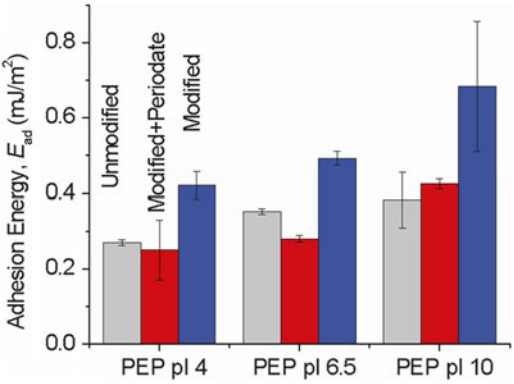

Fig. 6.5 The adhesion of three peptides after periodate modification are similar to the adhesion energy of three unmodified peptides. The adhesion energies are averaged from the values of 6–12 repeating force runs under each condition

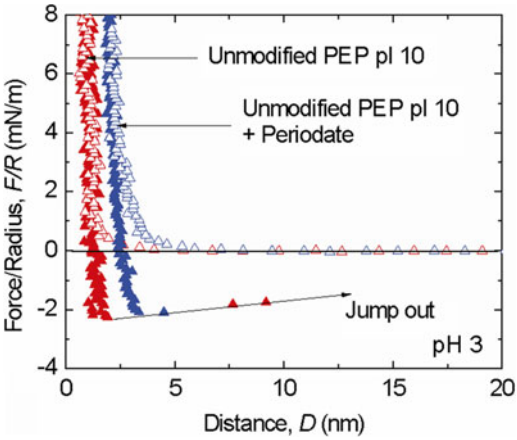

Fig. 6.6 The force-distance curves of unmodified PEP pI 10 before and after adding sodium periodate while remaining the pH unchanged (pH = 3). Adding sodium periodate does not change the adhesion force of unmodified PEP pI 10, although the hard wall slightly increased

6.5 Comparing Mfp-5-Derived Peptides to Mfp-5

All three Mfp-5-derived peptides showed adhesion energies that are at least an order of magnitude lower than the adhesion energy of intact Mfp-5, about 7.1 mJ/m^2 (adjusted according to the Derjaguin approximation $F/2\pi R$), measured by the SFA [6]. Mfp-5 consists of about 74 amino acid residues, 20 of which are Dopa (~30 mol% as per molecule) [14]. Given their size and flexible extended conformations, Mfp-5 molecules are likely to have worm-like structures on the mica surface. The long protein backbone and many Dopa side chains give Mfp-5 molecules an excellent opportunity to bridge two surfaces and with Dopa residues connected to the same peptide backbone firmly planted on both sides (Fig. 6.7a). The peptides, meanwhile, are much shorter, with between 3 and 5 Dopa groups in their sequence. During the deposition, a whole peptide molecule may stick to a single mica surface with most of Dopa residues bound to the same surface, leaving no or few Dopa

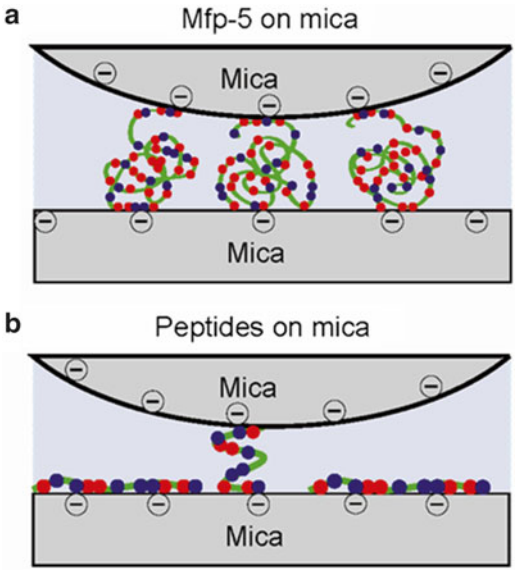

Fig. 6.7 A comparison of the binding models of Mfp-5 (**a**) and PEP pI 10 (**b**). The *red dots* represent Dopa and *blue dots* represent positive charge, both of which are involved in the binding of the peptides and possibly Mfp-5 on a mica surface

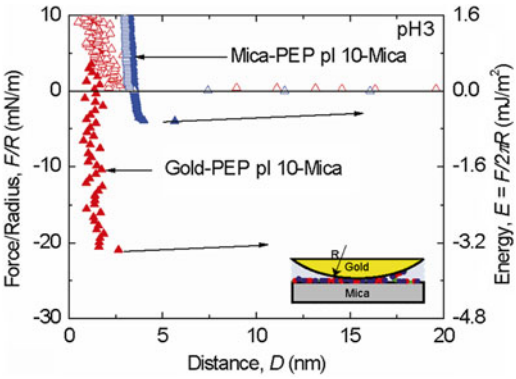

Fig. 6.8 The force-distance profile of PEP pI 10 coated on one mica surface against a gold surface. PEP pI 10 showed five times stronger adhesion force in comparison to the adhesion force between two mica surfaces

groups to bridge to the other mica surface and resulting in lower adhesion (Fig. 6.7b). This unevenly distributed Dopa binding is further suggested by the strong adhesion force (~3 mJ/m^2) of PEP pI 10 in a gold/peptide/mica geometry by measuring the adhesion force of a Pep pI 10 deposited mica surface against an opposing gold surface in pH 3 buffer (Fig. 6.8). On the peptide/gold interface, PEP pI 10 mainly interacts with the gold surface through the hydrophobic interaction or interactions between the charges on the peptide and the gold surface (the so-called image force), while no Dopa bridging is required [27]. This different binding mechanism gives PEP pI 10 a much higher chance to bridge the mica and gold surface, giving strong adhesion force. This high adhesion energy suggests the binding strength on the PEP pI 10/mica interface is at least, if no stronger than, 3 mJ/m^2, which is about 40 % of the value of Mfp-5 on the mica surface [6].

All three peptides show lower binding strength to mica surface; however, these simplified peptides allow us to investigate the effect of electrostatic interactions on the binding mechanism of the peptides, which was not previously detected in Mfp-5 by the SFA, possibly due to the steric effect of the native protein backbone [27]. The differences between Mfp-5 and the peptide adhesion demonstrate that peptide fragments of Mfp-5 cannot recapitulate the adhesion of the whole protein, e.g., there are synergistic effects from the amino acid residues across the whole protein sequence, which cannot be achieved by protein fragments. Given the fact that nature has optimized mussel proteins for adhesion over millions of years, these synergistic effects should not be so surprising. Taking short sequences from the mussel adhesive proteins, however, gives us a much simpler way to design better mussel-inspired adhesives and is more cost-effective from the engineering perspective.

References

1. Anderson TH et al (2010) Adv Funct Mater 20(23):4196–4205
2. Harrington MJ et al (2010) Science 328(5975):216–220
3. Holten-Andersen N et al (2011) Proc Natl Acad Sci U S A 108(7):2651–2655
4. Lee H, Scherer NF, Messersmith PB (2006) Proc Natl Acad Sci U S A 103(35):12999–13003
5. Zeng HB et al (2010) Proc Natl Acad Sci U S A 107(29):12850–12853
6. Danner EW et al (2012) Biochemistry 51(33):6511–6518
7. Lin Q et al (2007) Proc Natl Acad Sci U S A 104(10):3782–3786
8. Lu Q et al (2012) Biomaterials 33(6):1903–1911
9. Qin Z, Buehler M (2012) Appl Phys Lett 101(8):083702–083704
10. Yu J et al (2011) Nat Chem Biol 7(9):588–590
11. Yu J et al (2011) Adv Mater 23(20):2362
12. Matos-Perez CR, White JD, Wilker JJ (2012) J Am Chem Soc 134(22):9498–9505
13. You I et al (2012) Angew Chem Int Ed 51(25):6126–6130
14. Waite JH, Qin XX (2001) Biochemistry 40(9):2887–2893
15. Zhao H, Waite JH (2006) J Biol Chem 281(36):26150–26158
16. Lee, B.P., et al (2011) Ann Rev Mater Res 41:99–132
17. Lee H et al (2007) Science 318(5849):426–430
18. Park KM, Park KD (2011) J Mater Chem 21(40):15906–15908
19. Shafiq Z et al (2012) Angew Chem Int Ed 51(18):4332–4335
20. Wang JJ et al (2008) Adv Mater 20(20):3872
21. Kuang JH, Messersmith PB (2012) Langmuir 28(18):7258–7266
22. Dalsin JL et al (2003) J Am Chem Soc 125(14):4253–4258
23. Lee YH et al (2008) Adv Mater 20(21):4154
24. Brubaker CE, Messersmith PB (2011) Biomacromolecules 12(12):4326–4334
25. Krivosheeva O, Dedinaite A, Claesson PM (2012) J Colloid Interface Sci 379:107–113
26. Taylor SW (2002) Anal Biochem 302(1):70–74
27. Israelachvili JN (2011) Intermolecular and surface forces, 3rd edn. Academic, Burlington, MA, p 674

Index

J. Yu, *Adhesive Interactions of Mussel Foot Proteins*, Springer Theses,
DOI 10.1007/978-3-319-06031-6,